CANADIAN THESES

THÈSES CANADIENNES

NOTICE

The quality of this microfiche is heavily dependent upon the quality of the original thesis submitted for microfilming. Every effort has been made to ensure the highest quality of reproduction possible

If pages are missing, contact the university which granted the degree.

Some pages may have indistinct print especially if the original pages were typed with a poor typewriter ribbon or if the university sent us an inferior photocopy.

Previously copyrighted materials (journal articles, published tests, etc.) are not filmed.

Reproduction in full or in part of this film is governed by the Canadian Copyright Act, R.S.C. 1970, c. C-30.

AVIS

La qualité de cette microfiche dépend grandement de la qualité de la thèse soumise au microfilmage Nous avons tout fait pour assurer une qualité supérieure de reproduction

S'il manque des pages, veuillez communiquer avec l'université qui a conféré le grade

La qualité d'impression de certaines pages peut laisser à désirer, surtout si les pages originales ont été dactylographiées à l'aide d'un ruban usé ou si l'université nous a fait parvenir une photocopie de qualité inférieure

Les documents qui font déjà l'objet d'un droit d'auteur (articles de revue, examens publiés, etc) ne sont pas microfilmés.

La reproduction, même partielle, de ce microfilm est soumise à la Loi canadienne sur le droit d'auteur, SRC 1970, c C-30.

THIS DISSERTATION HAS BEEN MICROFILMED EXACTLY AS RECEIVED

LA THÈSE A ÉTÉ MICROFILMÉE TELLE QUE NOUS L'AVONS REÇUE

Canada

Analytical Modeling of the Responses of Ice-Covered Streams to A Thermal Effluent

Walid Saleh

A Thesis

in

The Department

of

Civil Engineering

Presented in Partial Fulfillment of the Requirements
for the Degree of Master of Engineering at
Concordia University
Montréal, Québec, Canada

March 1987

ISBN 0-315-35560-3

ABSTRACT

Analytical Modeling of The Responses of
Ice-Covered Streams to a Thermal Effluent

Walid Saleh

In many northern rivers, reaches of open water in the ice cover may exist throughout the winter season. Some of these reaches are the result of a tributary thermal effluent of higher temperature, or of fast moving water, that alters the thermal and hydrodynamic conditions of ice cover progression. Being mixed and dispersed within the receiving stream, the heat is eventually transfered to the atmosphere through evaporation, radiation, and conduction.

The temperature distribution, downstream of the point of effluent discharge, is determined by the hydrodynamic characteristics of the stream and by the prevailing meteorological conditions at the site. If sufficient heat is introduced into the receiving flow, the progression of ice cover may be completely halted over a large distance, mainly downstream of the discharge point, for the entire winter period.

This thesis deals with the development and testing of a special approach, based on perturbation techniques, concerned with the suppression of ice cover from the point of effluent discharge up to the ultimate advancing of its fronts. The mathematical formulation is based on the assumption that mixing of the tributary effluent with the receiving water body occurs both vertically and laterally at all sections of the stream, including at the location of discharge. The heat exchange terms in the governing equations are expressed as linear functions of the average temperature. Although the above theoretical formulation is based on a quasi one-dimensional

approach, it allows for special consideration of the non-linear variation in the stream geometry and adjustment for non-mixing assumption.

The formulation of the upstream ice edge location is developed based on the 0°C isotherm criterion. The upstream and the downstream ice edges are determined for unsteady uniform flow and for steady non-uniform flow. Conditions for the non-suppression of the ice cover are also obtained, based on the relative positions of the upstream and downstream ice edges. A comparison with field data shows good agreement with the formulation incorporating the flow velocity effect.

ACKNOWLEDGEMENTS

I take this opportunity to express my sincere appreciation to my thesis Advisor, Dr. Semaan Sarraf, for his indispensible support and helpful guidance which brought about the realization of this thesis.

Further thanks go to Mme. Danielle Zaikoff, directrice Construction, and Mr. Pierre Desroches, Engineer Projets Recherches, of HYDRO-QUEBEC, for the valuable information and field data which were necessary to carry out this work.

Beyond this, I express my deep indebtedness and admiration to my wife, France Cloutier, for her patience, stamina, and understanding throughout the preparation of this thesis.

I dedicate this thesis to the memory of my brother Mohammed for his support and encouragement, and for the love he gave me.....

TABLE OF CONTENTS

LIST OF SYMBOLS

Symbol		Description and Unit
C	=	empirical coefficient of the order of 0.023 used to calculate h_{wa}
C_a	=	specific heat of air under constant pressure
C_s	=	specific heat of snow
C_p	=	specific heat of ice = 1.0 cal g^{-1} °C^{-1}
D	=	flow depth in meters
E_x,E_z	=	longitudinal and transversal mixing coefficients respectively, in m^2sec^{-1}
E^*	=	equivalent retarding dispersion coefficient, in m^2/sec
E^l	=	longitudinal dispersion coefficient, in m^2/sec
E_1	=	specific humidity
E	=	apparent dispersion coefficient in $m^2.sec^{-1}$
e_{sw}	=	saturated vapour pressure in, (mb)
g	=	acceleration due to gravity
h_{wa}	=	heat-transfer coefficient at the water-air interface, in $w.m^{-2}$°C^{-1}

Symbol		Description
h_{wi}	=	heat transfer coefficient at the water-ice interface, in $w.m^{-2}\,°C^{-1}$
h_{ia}	=	heat transfer coefficient at the ice-air interface, in $w.m^{-2}\,°C^{-1}$
H_L	=	latent heat of fusion of ice
H_{LE}	=	latent heat of evaporation of water
h_i	=	ice cover thickness in, m
K	=	thermal conductivity of the ice in, $w\,m^{-1}\,°C^{-1}$
K_w	=	thermal conductivity of water in $w\,m^{-1}\,°C^{-1}$
K_C, K_E	=	turbulent diffusion coefficients for vapour and sensible heat respectively
P	=	atmospheric pressure, in (mb)
P_s	=	rate of snow fall per unit area, in $(g\,cm^{-2}\,hr^{-1})$
R	=	hydraulic radius, in meters
S_e	=	slope of the energy line
T_a	=	air temperature, in °C
T	=	water temperature, in °C

Symbol		Description
T_s	=	temperature of the top surface of the ice.cover, in °C
T_1	=	water temperature in channel-1, in °C
T_2	=	water temperature in the side channel, in °C
T_o	=	initial water temperature upstream of channel-1, in °C
T_o^*	=	mixing water temperature, in °C
T_e	=	water temperature at the ice edge
T_m	=	water temperature at water-ice interfac, in °C
t	=	time, in seconds
u,v	=	mean flow velocity components in the x (longitudinal) and in the z (transversal) directions respectively, in m s^{-1}
U^*	=	sheer velocity
u_c	=	initial flow velocity upstream of the point of discharge, in ms^{-1}
u_m	=	flow velocity at the mixing section, in m s^{-1}
V_{a2} , e_{a2}	=	wind velocity in, m/sec, and the vapour pressure ie, (mb).
x_o	=	datum reference point on channel-1, in m

Symbol		Description
x_u	=	upstream ice edge location, upstream of the point of discharge, in m
x_m	=	location of the mixing section, in m
x_d	=	downstream ice edge location downstream of the point of discharge, in m
ρ	=	density of water, in kg m^{-3}
ρ_a	=	air density, in Kg m^{-3}
ε	=	emissivity of the water surface=0.97
μ	=	dynamic viscosity, in kg m^{-1} s^{-1}
γ	=	psychometric constant in Bowen-Ratio
σ	=	Stefan-Boltzman constant =$4.879*10^{-9}$ cal.m^{-2} hr^{-1} $K^{\circ-4}$
Φ	=	heat flux at the water-air or water-ice interface
Φ_{wa}	=	heat flux at the water-air interface
ϕ_{wi}	=	heat flux at the water-ice interface
Φ_i	=	heat flux through ice sheet
ϕ_R	=	heat flux due to solar radiation

Symbol		Description
ϕ_B	=	heat flux due to long-wave radiation
Φ_{CL}	=	incoming clear sky radiation
ϕ_E	=	evaporative heat flux
Φ_{rr}	=	reflected short-wave radiation
ϕ_H	=	conductive heat flux
Φ_{ba}	=	intensity of long-wave radiation that will reach the water surface

LIST OF FIGURES

LIST OF TABLES

CHAPTER 1

INTRODUCTION

1.1 Preface

The study of the thermal responses of ice-covered streams to an effluent of high temperature, or of fast moving water, has been of considerable interest to those concerned with hydraulic systems, environmental effects, and navigational routes in cold regions.

Power plants and other industries, for obvious economic reasons, normally dispose of their heated waste water into nearby streams . This practice has always been considered an acceptable economic and social compromise between environmental protection, consumptive water use, and energy production. However, concerns have recently been raised about its effect on the aquatic environment and on the overall ecological balance. The undesirable changes in the physical properties of water caused by the waste heat disposal have led to the imposition of maximum temperature incrases by concerned authorities.

In northern rivers, and in the presence of a tributary effluent of relatively high temperature or of fast moving water, the ice cover is usually suppressed in the receiving reach in the vicinity of the point of discharge. If sufficient heat were introduced into the receiving flow, the ice cover might melt completely over a large distance, essentially downstream of the discharge point, for the entire winter period. In navigable rivers, proper positioning of the heated side effluent might permit an effective use of rivers for shipping throughout the winter period. For instance, in Canada, the St. Lawrence Seaway closes annually from January to March , inflicting a high cost on the Canadian economy.

Preventing the formation of ice cover, or decreasing its thickness during the winter

months, may also reduce the chance of floods caused by ice jams. On the other hand, open water reaches in ice-covered rivers could, under severe atmospheric conditions, produce large quantities of frazil ice. The latter is responsible for an increase in the stream head loss; up to 25% has been recorded [2].

For the reasons mentioned above, it has become necessary for hydraulicians to study and predict the thermal behaviour of streams subjected to a tributary thermal effluent. The magnitude and extent of changes in the river temperature distribution due to a thermal side effluent input depend mainly upon the degree of mixing between the warm effluent and the cooler receiving flow, as well as on the rate of heat exchange between water and atmosphere. The mixing process is dominant only in the region adjacent to the point of thermal discharge. Downstream from this area, the water temperature distribution is controlled by the prevailing surface heat exchange. The net amount of heat transferred from the water to the atmosphere is controlled by various processes, which depend on climatological conditions. Heat budget items, associated with short-and long-wave radiation, evaporation and convection to the atmosphere, are considered here.

1.2 Literature Review

Early attempts to study the problem have focused on estimating the temporal, rather than the spatial changes in temperature in a reach. Ince and Ashe [22] used field data from the St. Lawrence river in order to compare two finite difference approaches to calculate the downstream water temperature attenuation. The evaluation of the length of the ice-free reach was first attempted by Dingman et al. [17]; they used a differential approach for the steady-state heat with constant meteorological conditions. Paily et al. [31,32] introduced generalized relationships between the major climatological factors and the coefficients of the

linearized heat loss by means of a multiple-regression analysis. In addition, their work included a derivation of a closed form solution of the unsteady, one-dimensional, convection-diffusion equation. Ashton [7] developed a quasi-steady numerical simulation that predicts the varying open water reach as a function of the tributary thermal load to the river, the atmospheric conditions, and the characteristics of the river flow. However, stream velocity was considered constant. Ashton [7,9] introduced a new criterion for the location of the ice edge, based on the heat balance at the undersurface of the ice cover. However, at a later stage, it was concluded that the 0 °C isotherm criterion provides a better prediction of the length of the ice free reach [10].

1.3 Research Objectives

In the present work, the phenomenon of ice cover suppression by a thermal side effluent is examined through an analytical model of which the unsteady-state quasi-linear energy equation forms the theoretical basis. An adequate formulation of the energy transfer process, related to the melting and freezing of the ice cover, was also incorporated. The model is designed to evaluate the dominant variables which govern the local melting of the ice cover in order to predict the occurrence of ice cover suppression through a new proposed criterion, and to estimate the location of both the upstream and downstream ice cover edges, for various hydrodynamic and meteorological conditions. It also addresses the variability of the flow velocity on the ice cover progression or regression in conjunction with a thermal effluent release. The equations were solved for the case of specific, as well as general, velocity variations. Perturbation techniques were used based on WKB approximation and Louville-Green transformation. In this manner, it was possible to account for the effect of the longitudinal diffusion, in addition to the flow velocity variability.

CHAPTER II

MATHEMATICAL FORMULATION

2.1 Governing Equations:

The mathematical representation of the thermal state of a stream is based on the principle of conservation of heat transported and dispersed by the flow. It describes the space-time distribution of the temperature as a function of the flow properties.

For an incompressible turbulent flow, the conservation law of thermal energy in a spatially variable river flow, under the conditions of uniform temperature distribution over the depth, can be expressed by the following partial differential equation:

$$\frac{\partial}{\partial t}(\rho C_p DT) + \frac{\partial}{\partial x}(\rho C_p DuT) + \frac{\partial}{\partial z}(\rho C_p DvT) = \frac{\partial}{\partial x}\left[DE_x \frac{\partial}{\partial x}(\rho C_p T)\right] + \frac{\partial}{\partial z}\left[DE_z \frac{\partial}{\partial z}(\rho C_p T)\right] - \Phi \qquad (2.1)$$

where D = the flow depth in (m); T = the water temperature (°C); u,v = the mean flow velocity components in the x (longitudinal) and in z (transverse) directions respectively in ms^{-1}; E_x, E_z = the longitudinal and transverse mixing coefficients respectively; C_p is the specific heat, and Φ = the heat flux at the water/air or water/ice interface. It is assumed that there is no heat flux at the river bed.

If, ρ, C_p and D are assumed to be constant, the above equation can be written as:

$$\frac{\partial T}{\partial t} + u\frac{\partial T}{\partial x} + v\frac{\partial T}{\partial z} = E_x \frac{\partial^2 T}{\partial x^2} + E_z \frac{\partial^2 T}{\partial z^2} - \frac{\Phi}{\rho C_p D} \qquad (2.2)$$

Also, the fact that [v ∂T/∂z] is of much lower order than [u ∂T/∂x] permits the omission of [v ∂T/∂z] term from the equation. In addition, the assumption of full mixing of the water temperature over the cross-section allows for the elimination of [E_z $\partial^2 T/\partial z^2$] term. Over a relatively small reach, the longitudinal dispersion coefficient remains invariant along the river reach. The final form of the one dimensional quasi-linear equation can be written as:

$$\frac{\partial T}{\partial t} + u \frac{\partial T}{\partial x} = E_x \frac{\partial^2 T}{\partial x^2} - \frac{\Phi}{\rho C_p D} \qquad (2.3)$$

This equation expresses an interrelated equilibrium among four major processes of heat transfer, which control the stream heat balance.These processes are represented by the following terms:

1. $\partial T/\partial t$; the rate of change of heat in a local water section;
2. $u\ \partial T/\partial x$; the advection of the heat at mean flow velocity;
3. $E_x\ \partial^2 T/\partial x^2$; the heat dispersion in the longitudinal direction;
4. Φ ; the rate of heat transfer at the water/ice or water/air interface.

The presence of u as a function of x gives this equation a quasi-linear form which requires advanced analytical techniques for its integration.

2.2 Rate of Heat Transfer, Φ:

For a fully mixed stream, the temperature distribution resulting from the discharge of the heat effluent is controlled by the rate of surface heat exchange. The latter is determined by different heat transfer processes, which depend upon a number of climatological factors.

When the air temperature is much lower than the water temperature, the water body

loses heat to the atmosphere, leading to a significant cooling of the water.

For the analysis of the heat transfer process, a definition sketch is presented in Fig. (2.1. a-b), for both open and ice-covered water.

2.2.1 Rate of Heat Transfer For Open Water Conditions:

When the top surface of the flow is open to the atmosphere, the heat flux Φ is denoted by Φ_{wa} (water-air interface). The heat flux at the water surface, Φ_{wa}, is a function of different heat transfer processes and can be expressed as follows:

$$\Phi_{wa} = \Phi_R - (\Phi_B + \Phi_E + \Phi_H + \Phi_S) \qquad (2.4)$$

where ;

Φ_R : solar or short wave radiation;

Φ_B : long wave radiation;

Φ_E : evaporative heat flux;

Φ_H : convective and conductive heat flux;

Φ_S : heat transfer rate during the melting of snow falling on the water surface.

During winter periods, where the air temperature T_a is lower than the water temperature, T, Φ_{wa} (heat flux at the water-air interface) is negative, and the water body is losing heat to the atmosphere. The major climatic factors contributing to and affecting the process are: the atmospheric pressure, air humidity and temperature, wind velocity, short and long wave radiations, and precipitation (especially snow). In the following, each component of the surface heat transfer components will be discussed and evaluated.

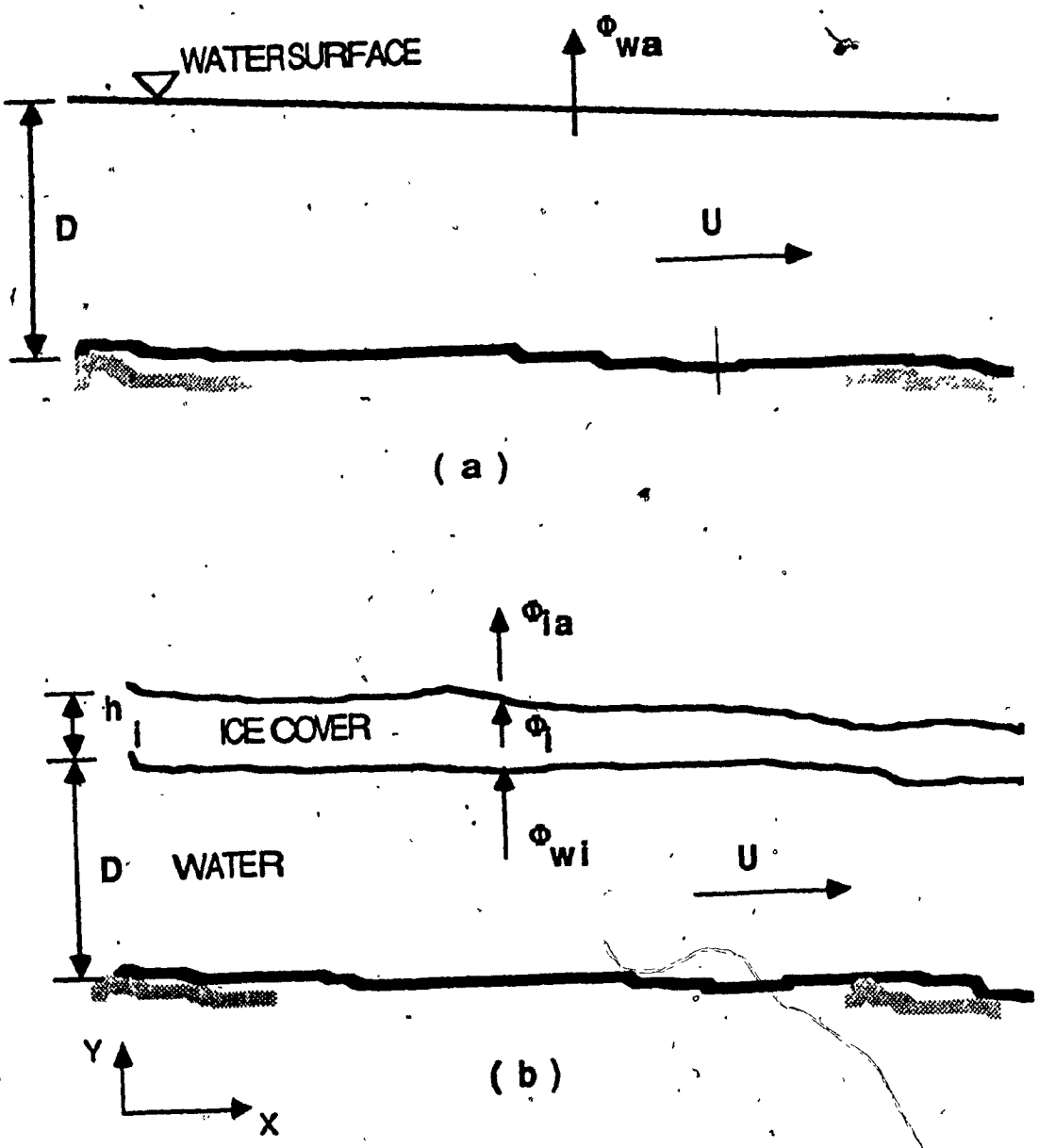

Fig: (2.1) Diagram of major heat transfer processes at the water surface:
a)without ice cover; b)with ice cover.

-Solar Wave Radiation:

The intensity of solar energy reaching the outer surface of the earth is 120 cal $cm^{-2}hr^{-1}$ if the surface is normal to the sun ray. When reaching the earth's surface, however, the intensity of the solar radiation is less than the above amount because of atmospheric absorption and because, in general, the earth's surface is at an angle to the sun's rays. Hence for different cloud-covered conditions, the combined, direct and indirect radiation "insolation Φ_I" is expressed by the following equation:

$$\Phi_I = \Phi_{CL} \{0.35 + 0.061 (10 - C)\} \qquad (2.5)$$

where Φ_{CL} is the incoming clear sky insolation, and C is cloud coverage in tenths (ranging from 0 for clear sky, to 10 for a completely overcast sky). Although the solar heat flux Φ_I reachs the water surface, a fraction Φ_{rr} is reflected back into space. Therefore Φ_R is the difference between the incident Φ_I and the reflected Φ_{rr} short-wave radiation, which can be represented mathematically as follows:

$$\Phi_R = \Phi_I - \Phi_{rr}$$

and $$\Phi_{rr} = 0.018\,\Phi_I - 6.766 \times 10^{-5}\,\Phi_I^2 \qquad (2.6)$$

-Long Wave Radiation Heat Flux Φ_B :

The net long-wave radiation heat loss to the water body is the difference between the long-wave radiation emitted by the water and the atmosphere. According to the Stefan-Boltzman

law, the heat flux emitted by the water surface is given by:

$$\Phi_{bw} = \varepsilon \sigma T^4 \quad (2.7)$$

where ε is the emissivity of the water surface and is equal to 0.97 Anderson [1], σ is the Stefan-Boltzman constant of 4.879×10^{-9} cal cm^{-2} hr^{-1} K$^{\circ}$ $^{-4}$, and T is the water surface temperature in K$^{\circ}$. The intensity of the long-wave radiation emited by the atmosphere that will reach the water surface under cloudy conditions, may be calculated from the following empirical equation Anderson [1]:

$$\Phi_{ba} = (a + be_a) \sigma T_a^4, \text{ cal cm}^{-2} \text{ hr}^{-1} \quad (2.8)$$

with $a = 0.74 + 0.025\ C \exp(-1.92 \times 10^{-4}\ H)$

and $b = 4.9 \times 10^{-3} - 5.4 \times 10^{-4}\ C \exp(-1.97 \times 10^{-4}\ H)$ (2.9)

where H is the height of the cloud in meters above 500 m. For a cloud height less than 500 m, H = 500 m is used. Therefore, the net long-wave radiation Φ_B can be presented mathematically as follows: $\Phi_B = \Phi_{bw} - \Phi_{ba} + \Phi_{ar}$.

As Φ_{bw} is nearly constant, the variation of Φ_B is determined by the variation of Φ_{ba}.

-Evaporative Heat Flux Φ_E and Convective and Conductive Heat Flux Φ_H :

The convective heat transfer, between the water and the air, depends on the temperature difference between the water and the air, and on the surface wind velocity. Therefore, the convective heat transfer process can be divided into natural and forced convection. When there is no wind, the natural convection by circulation that is set up by the temperature difference is dominant. However, in the presence of a strong wind, the eddies in the flow field also help to transport the heat, and the heat transferred due to forced convection is

dominant. Under forced convection conditions, the evaporative heat transfer and the convective (sensible) heat transfer are governed by the following diffusion equations:

$$\Phi_E = -K_E \rho_a H_{LE} (dE_1 / dY) \quad (2.10)$$

and $$\Phi_H = -K_C \rho_a C_a (dT_a / dY) \quad (2.11)$$

where E_1 is the specific humidity (the ratio of the mass of water vapour to the mass of dry air in a given volume of mixture), Y is the vertical direction, ρ_a is the density of the air, C_a is the specific heat of air under constant pressure, H_{LE} is the latent heat of evaporation of water and K_E, K_C are turbulent diffusion coefficients for vapour and sensible heat respectively. The ratio of Φ_H/Φ_E is known as the Bowen ratio R.

If the transport mechanism of the vapour is assumed to be the same as the transport mechanism of the air itself, then K_E and K_C will be equal, and from eqs.(2.12) and (2.13), evaluated between the water surface and the atmosphere. After appropriate conversion constants are substituted, one obtains Dingman [17]:

$$R = 6.1 \times 10^{-4} P [T-T_a/e_{sw}- e_a] \quad (2.12)$$

where P is the atmospheric pressure in millibars, and e_{sw} is the saturated vapour pressure at T, also in millibars.

There are many empirical equations for calculating the evaporative heat loss; Dingman [17] presented an equation for Φ_E as follows:

$$\Phi_E = (0.131 + 0.306\ V_{a2}) (e_{sw}- e_{a2})\ \text{cal cm}^{-2}\,\text{hr}^{-1} \quad (2.13)$$

where V_{a2} and e_{a2} are the wind velocity (m/s) and the vapour pressure (mb) at a height of 2m respectively. The general approach to calculate Φ_H is by multiplication of Eqs. (2.12) and (2.13), and with the approximation that P = 1000 mb gives:

$$\Phi_H = (0.080 + 0.186\ V_{az})\ (T - T_a) \quad \text{cal cm}^{-2}\ \text{hr}^{-1} \qquad (2.14)$$

It should be noted that in the above empirical equations, the direction of the wind is not considered as a parameter.

-Heat Flux as a Consequence of Precipitation, Φ_S:

The heat transfer rate, as a result of the melting of snow falling on the water surface, can be noted as Φ_S. From the conservation of heat, the heat flux, Φ_S, for heating up and melting snow, is given by:

$$\Phi_S = P_s\ (H_L + C_S\ (T - T_S)\ ) \qquad (2.15)$$

where P_s is the rate of snowfall per unit area (g $\text{cm}^{-2}\ \text{hr}^{-1}$), H_L is the latent heat of fusion of ice, C_S is the specific heat of snow, and T_s is the temperature of the snow. Although precipitation has been identified as a component of the total heat transfer, the contribution due to snowfall is not substantial compared to the total heat loss of the season, Freysteinsson[23].

Table [2.1] Asvall [11] gives the total heat loss rate at the water surface at different wind speeds, different cloud coverages, and different air temperatures. The table was constructed based on measured data from Norway (APPENDIX).

Because the surface heat exchange rate, $\Phi_{wa}(T)$, appears to be a complex function of

the water temperature, attempts have been made to express it as a linear function of the water temperature.

The existing linearized models are due to Edinger, Duttweiler and Geyer [20], Yotsukura, Jakman and Faust [41]. Paily, et al.[31] introduced a linearization of the surface heat exchange relation, which approximates Φ_{wa} by:

$$\Phi_{wa} = -\varepsilon (T + \eta / \varepsilon) \qquad (2..16)$$

where η = a base heat exchange rate corresponding to a stream temperature of 0°C; and ε = the coefficient of the heat exchange. The linearized values of ε and η were represented by:

$$\varepsilon = a + b (V_{a2}) + C (T_{a2}) + d(R.H) + e (V) \qquad (2.17)$$

with a = 30.03958; b = 7.07423; c = 1.04632; d = -0.01656, and e = -0.01093, ε in cal cm^{-2} day^{-1} $°C^{-1}$

and: $\eta = \eta^1 - \Phi_R$

where η^1 is the base heat exchange rate without the net solar radiation. The value of η^1 was represented by:

$$\eta^1 = 291 + 29.3 (V_a) - 18.7 (T_a) - 1.75 (R.H) - 1.02(V) - 4.58 (V_a T_a) - 0.184$$

$$(V_a * R.H) - 0.111 (T_a * R.H) + 0.153 (T_a^2) - 0.496 (R.H)$$

for clear skies. The range of all the variables involved is: 1. ($0 \le V_a \le 12$, m sec^{-1});

2. ($-21 \le T_a \le 0$, °C); 3. ($0 \le R.H \le 100$, tenth); 4. ($1 \le V \le 10$, KM).

In the present study, it is assumed that the wind velocity, V_w, and air temperature,

T_a, are the dominating climatological factors. Hence Φ_{wa} is expressed by the following relationship:

$$\Phi_{wa} = h_{wa} (T - T_a) \qquad (2.18)$$

where h_{wa} is the heat transfer coefficient applied to the difference between the water temperature T and the ambient air temperature T_a. This coefficient (h_{wa}) is largely dependent on the wind velocity, expressed generally by:

$$h_{wa} = a + b V_w \qquad (2.19)$$

where a is the heat transfer coefficient for still air, and bV_w is the wind effect with V_w the ambient wind velocity measured at some specified height above the surface [7]. For a wind with an approximate velocity of 4.5 m sec^{-1} the value of $h_{wa} = 25$ w $m^{-2} \cdot C^{-1}$.

2.2.2 Rate of Heat transfer For Ice Cover Conditions :

Under ice cover conditions, the heat flux consists of three major processes as shown in Fig (2.1). The heat flux to the atmosphere (at the ice-air interface during ice growth) is formulated as:

$$\Phi_{ia} = h_{ia}(T_s - T_a) \qquad (2.20)$$

where h_{ia} is the heat transfer coefficient at the ice-air interface in ($W.m^{-2}.C^{-1}$), T_s and T_a are the ice surface and the air temperatures ($^{\circ}C$) respectively. This is a simplified model and the heat transfer coefficient encompasses several heat transfer budget components and wind velocity.

During the ice cover growth, the conductive heat flux through the ice sheet , assuming a linear temperature profile in the ice cover, is :

$$\Phi_i = k\,(T_m - T_s)/h_i \qquad (2.21)$$

where k is the thermal conductivity ($W.m^{-1}.\,^{\circ}C^{-1}$) of the ice, T_m is the melting temperature of the ice ($^{\circ}C$), and the net heat flux is zero.

If the assumption is made that evaporative and condensation losses are minimal at the ice-atmosphere interface, with the existence of a steady-state condition, then $\Phi_{ia} = \Phi_i$, which allows T_s to be eliminated, and the heat transfer rate through the ice sheet can be represented by:

$$\Phi_i = (T_m - T_a)/(h_i/k + 1/h_{ia}) \qquad (2.22)$$

In general, for the ice-covered flow, the heat flux Φ_{wi} at the water-ice interface is the dominant process which depends on the flow hydrodynamic variables, and can be expressed as follows [7]:

$$\Phi_{wi} = h_{wi}(T - T_m) \qquad (2.23)$$

where h_{wi} is the heat transfer coefficient ($w.m^{-2}.^{\circ}C^{-1}$); T_m and T are the melting point ($T_m = 0^{\circ}C$) and the water temperature respectively. The classical approach to evaluate h_{wi} is based upon a closed conduit turbulent heat transfer correlation [33], which is given by the following formula:

$$\frac{h_{wi}\,R}{k_w} = C\left(\frac{u\,R\rho}{m}\right)^{0.8}\left(\frac{\mu\,C_p}{k_w}\right)^{0.4} \qquad (2.24)$$

where R: the hydraulic radius (m); u: the mean flow velocity (ms^{-1}); ρ: the density(kgm^{-3});

μ: the dynamic viscosity ($kgm^{-1}s^{-1}$); C_p: the specific heat ($kg^{-1}\ °C^{-1}$); K_w: the thermal conductivity of water ($wm^{-1}°C^{-1}$); C: an empirical coefficient of the order of 0.023 Rohsenow and Choi, [33]. By evaluating the above thermal properties at 0°C and R = D/2 ,we get,

$$h_{wi} = C_{wi} \frac{u^{0.8}}{D^{0.2}} \qquad (2.25)$$

where: $C_{wi} = 1622\ ws^{0.8}m^{-2.6}\ °C^{-1}$ for C = 0.023 and

$C_{wi} = 2433\ ws^{0.8}m^{-2.6}\ °C^{-1}$ for C = 0.0345

2.3 Longitudinal Dispersion Coefficient, E:

The longitudinal dispersion coefficient is influenced mainly by the combined mechanisms of mixing over the flow cross section and the variation of the longitudinal velocity within the flow cross section. Major studies in longitudinal mixing have been done by Fisher [24,25], Sayre [34], Carter and Okubo [13]. However, based on laboratory investigation of longitudinal dispersion in open channel flows and field measurements in natural streams, formulas have been developed to predict the longitudinal dispersion coefficient. The most common formula is expressed by:

$$E = C\ D\ U^* \qquad (2.26)$$

where C is a constant, D is the depth of flow, or the width of channel, and $U^* = \sqrt{RgS_e}$ is the shear velocity, in which R is the hydraulic radius, g is the acceleration due to gravity, and S_e is the slope of the energy line. Investigations have yielded values of C ranging from 5 to 7500. Fisher [25] has summarized these values in a tabular form, which is presented in Table [2.2] (APPENDIX).

CHAPTR III

Ice Cover Response to Heat Transport by Advection

For the purpose of analysis, the configuration of the channel intersection shown in Fig. (3.1.a-b) is considered. The main channel-1 is assumed to be narrow and covered with ice, except in the vicinity of the intersection, if conditions are favourable. The water temperature is assumed uniform over the cross-section. T_1 °C is the water temperature in channel-1, and [$T_2 > T_1$] is the water temperature in channel-2. At the intersection, the ice cover may be suppressed in the main channel and an open water area might occur mainly downstream of the point of side effluent discharge.

The main purpose of this chapter is to identify the dominant variables, and their values, for which the ice cover will be suppressed, and consequently, to evaluate the upstream and the downstream ice cover edges. It will also be a question of response of the ice edge location to changes in the meteorological variables and discharges.

3.1 Uniform Flow Case:

For the unsteady state uniform flow, with constant velocity along channel-1, the longitudinal mixing term [$E_x \partial^2T/\partial X^2$] may be neglected. Hence, the dispersion process is presumably accomplished through advection in the direction of the main flow. Therefore, equation (2.3) can be reduced to:

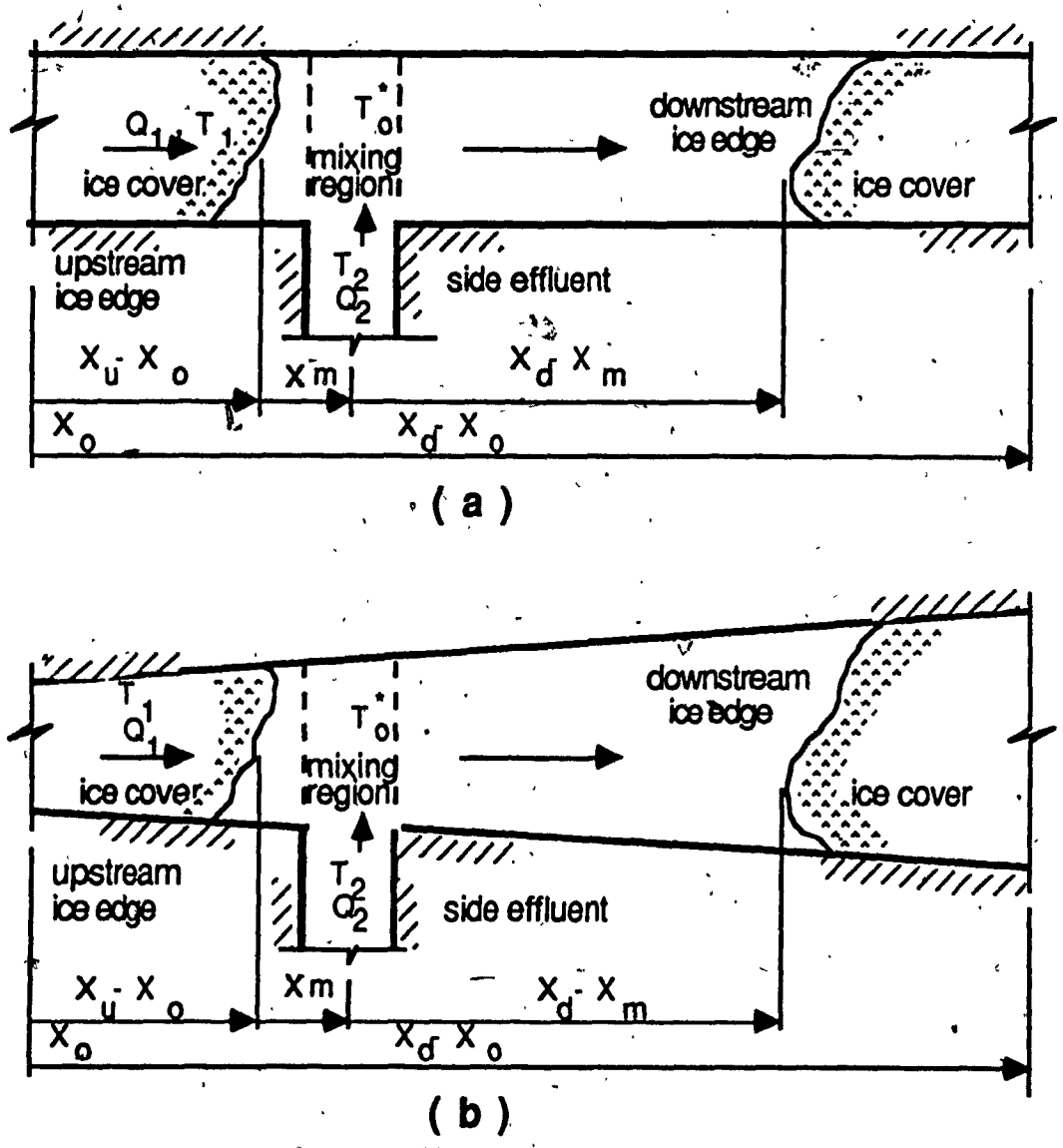

Fig: (3.1) Channel configuration with various geometrical locations.

a) Constant width channel; b) Variable width channel.

$$\frac{\partial T}{\partial t} + u \frac{\partial T}{\partial x} = - \frac{\Phi}{\rho C_p D} \qquad (3.1)$$

In the following section we will solve this equation for both upstream and downstream reaches of the river from the point of discharge.

3.1.1 For Ice-Covered Reach (upstream of the point of discharge)

Under ice-covered conditions, Φ_{wi} can be expressed according to equation [2.25]. In order to solve equation [3.1], a new transformation has been introduced:

$$\xi = \xi\ (x,t) = x + ut \qquad (3.2)$$

Where $[\partial\xi/\partial x] = 1$; and $[\partial\xi/\partial t] = u$, and

$$\frac{\partial T}{\partial t} = \frac{\partial T}{\partial \xi} \frac{\partial \xi}{\partial t} = u \frac{\partial T}{\partial \xi}$$

$$\frac{\partial T}{\partial x} = \frac{\partial T}{\partial \xi} \frac{\partial \xi}{\partial x} = \frac{\partial T}{\partial \xi} \qquad (3.3)$$

and in terms of the new variable ξ, equation (3.1) can be written as follows:

$$\frac{\partial T}{\partial \xi} = \frac{1}{2 u \rho C_p D} h_{wi} (T - T_m) \qquad (3.4)$$

Solving for the boundary conditions that at $x = x_o$, $T_1 = T_o$; & at $x = x_u$, $T_1 = T_m$, the final solution is given by :

$$\frac{T_1 - T_m}{T_o - T_m} = \text{Exp} \left[\frac{2 \rho C_p D u}{h_{wi}} (x - x_o) \right] \qquad (3.5)$$

At the intersection, the water is assumed to be fully mixed. The resulting mixing temperature T_o^* °C can be given by:

$$T_o^* = \frac{T_1 Q_1 + T_2 Q_2}{Q_1 + Q_2} \tag{3.6}$$

where Q_1, Q_2 are the flow rate in channel-1 and channel-2, respectively; T_1, and T_2 are as defined earlier.

3.1.2 Open Water Reach (downstream of the point of discharge)

The heat transfer rate Φ is given by equation (2.18), in the following form:

$$\Phi = \Phi_{wa} = h_{wa} (T - T_a)$$

By inserting it in equation (3.1) and applying the previous transformation, the following solution will result from the integration:

$$\frac{T_e - T_a}{T_o^* - T_a} = \text{Exp}\left[\frac{-h_{wa}}{\rho C_p D u} (x_e - x_m)\right] \tag{3.7}$$

for the boundary conditions that at $x = x_m$, $T = T_o^*$. The location of the ice cover edge according to the 0 °C isotherm criterion is given by:

$$(x_d - x_m)/T_{e=0} = -\frac{\rho C_p D u}{h_{wa}} \text{Log}_e \left[\frac{-T_a}{T_o^* + T_a}\right] \tag{3.8}$$

where T_e is the water temperature at the ice cover edge, assumed to be zero.

3.1.3 Open Water case (upstream of the point of discharge)

Upstream of the point of discharge, a relatively small open water area is usually encountered as a result of the migration of warm thermal effluent in the upper layer of the stream. Due to the fact that the effluent is warmer than the ambient river water temperature, a stratification and a partial upstream flow is established in the upper layer of the stream, adjacent to the ice cover. In the present study, this phenomenon can be regarded as a heat diffusion process in the upstream direction. The retarding effect of the main flow is accounted for through the introduction of an apparent dispersion coefficient that is:

$$\bar{E} = E - E^*$$

where E^* is the equivalent retarding dispersion coefficient estimated by the transport term, assuming that:

$$\frac{\partial}{\partial x}\left(uT\right) = \frac{\partial}{\partial x}\left(E^* \frac{\partial T}{\partial x}\right) \qquad (3.9)$$

which leads to:

$$E^* = \frac{uT}{\partial T / \partial x} = \frac{uT}{G_T} \qquad (3.10)$$

where G_T is a nominal temperature gradient which depends on the configuration of the channel intersection, and can be evaluated from field data. Hence, in the open water reach upstream of the point of discharge, the energy balance can be formulated as follows:

$$\bar{E}\frac{\partial^2 T}{\partial x^2} = \frac{\Phi}{\rho C_p D} = \frac{h_{wa}}{\rho C_p D}\left(T - T_a\right) \qquad (3.11)$$

Solving this equation for the following boundary condition, at $x = x_m$, $T = T_o^*$, & at $x = x_o$, $T_1 = T_o$, the final solution yields:

$$(x_u - x_m) = \frac{\log_e \left[\frac{T_e - T_a}{T_o - T_a} \right]}{\left[\frac{h_{wa}}{\rho C_p D \overline{E}} \right]^{1/2}} \qquad (3.12)$$

where x_u: is the upstream ice edge location; x_m, the point of discharge; T_e: the water temperature at the ice edge, assumed to be zero according to the 0 °C isotherm criterion. This equation represents the location of the upstream ice cover edge, and it is shown in Fig. (3.2) for flow depth of 5 m. The convective heat transfer term is neglected, since the relative velocity of the water flowing upstream in the upper layer, is practically nil.

3.2 Steady non-uniform flow:

In this case, the equation was solved for a steady non-uniform flow, with variable velocity u being considered as a function of the x coordinate. Using the same assumptions as in the previous case, and considering each term as daily averaged values, equation (2.3) becomes:

$$u(x) \frac{\partial T}{\partial x} = \frac{-\Phi(T)}{\rho C_p D} \qquad (3.13)$$

For a known form of the expression of u as a function of x, the above equation can be integrated either analytically or numerically.

In the following section the above equation will be solved for both upstream and downstream reaches of the river from the point of discharge.

3.2.1 For ice-covered reach (upstream of the point of discharge)

Assume the velocity u = u(x) is considered to vary according to the following relation:

$$u = k(x - x_o) + u_o$$

where u_o = is the initial water velocity (m/sec)at $x=x_o$

$$k = \frac{-k_1}{\rho C_p D^{1.2}} \quad ; \quad k_1 = 1622\ ^{\circ}C S m^{-0.2} \text{ jol.}^{-1}$$

The solution for the boundary condition at $x = x_o, T_1 = T_o$, can be expressed as follows:

$$\frac{T_1 - T_m}{T_o - T_m} = \text{Exp}\left[\frac{1}{0.8}\left\{ k\left(x - x_o\right) + u_o\right\}^{0.8} - u_o^{0.8}\right] \qquad (3.14)$$

This equation represents the water temperature attenuation under the ice cover for variable flow velocity, and it is shown in Fig. (3.3).

3.2.2 Open water reach (downstream of the point of discharge)

For the open-water reach, the heat transfer rate Φ is given by equation (2.18) in the form:

$$\Phi = \Phi_{wa} = h_{wa} (T - T_a)$$

for a velocity which is assumed to vary linearly with respect to x, such as:

$$u = k' (x - x_m) + u_m$$

Integration of equation (3.13), for the boundary conditions that at $x = x_m$, $T = To^{\circ}$, yields:

$$\frac{T_e - T_a}{T_o^{\circ} - T_a} = \frac{K'(x_d - x_m) + u_m}{u_m} \qquad (3.15)$$

where: $K' = 30/\rho C_p D$

The location of the ice cover edge according to the 0°C isotherm is therefore given by:

$$(x_d - x_m)_{T_e = 0} = \frac{u_m}{K'}\left(\frac{T_m - T_a}{T_o^{\circ} - T_a} - 1\right) \qquad (3.16)$$

The formulation of $(x_u - x_m)$ has not changed in this case, since the velocity effect is negligible. The downstream locations for both constant and variable velocity conditions, as described by equation (3.8) and equation (3.16), are shown in Fig.(3.4). The comparison between the formulations for temperature attenuation and those given in previous works is shown in Fig. (3.5).

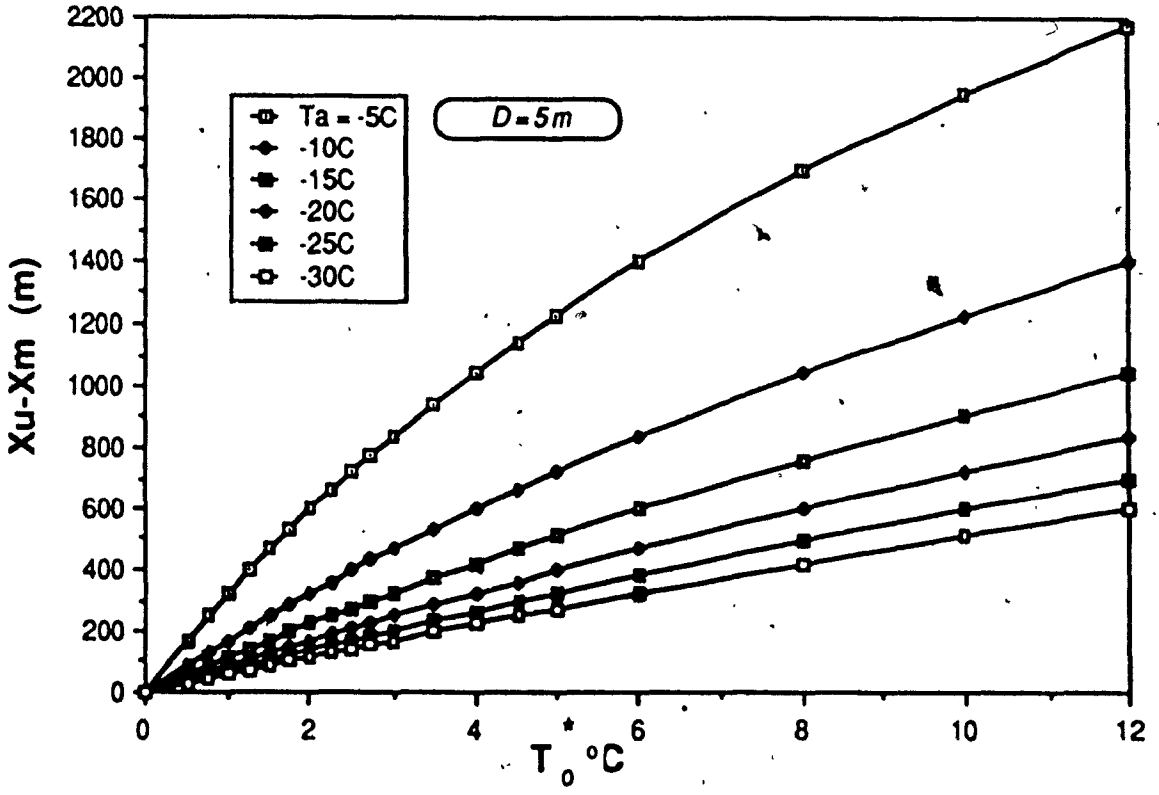

Fig. (3.2): Upstream location of the ice edge for a uniform flow depth of:

D = 5 m.

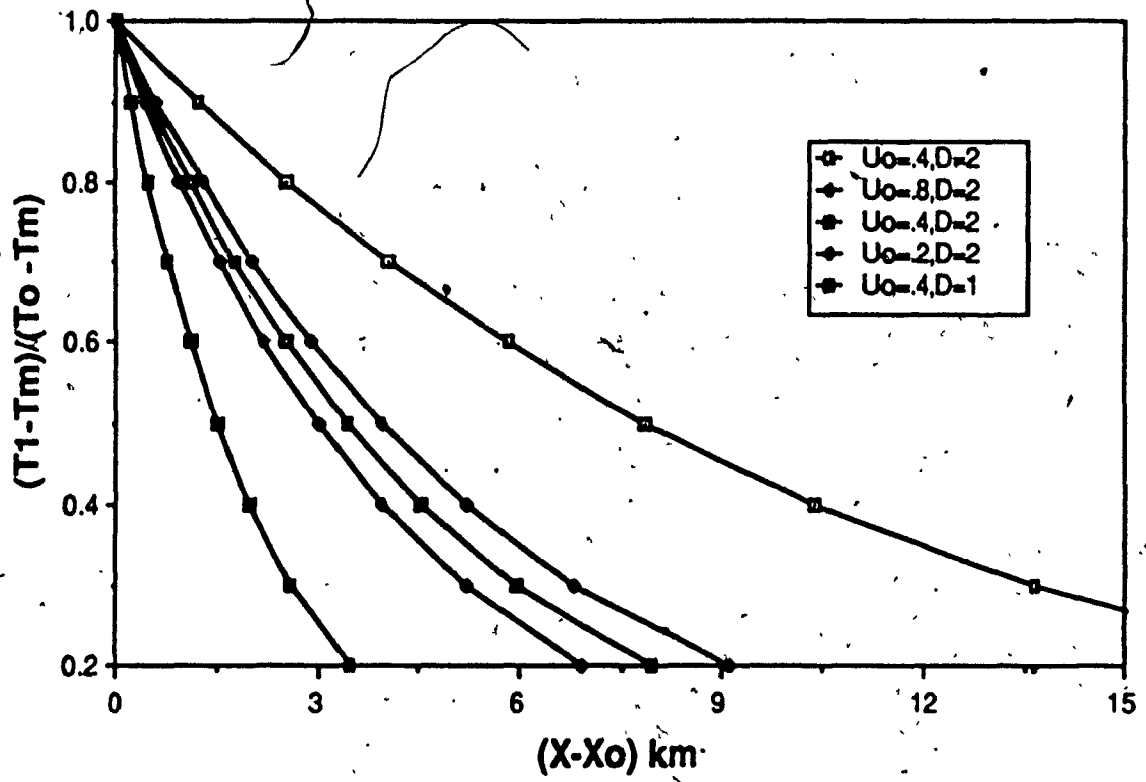

Fig: (3.3) Calculated water temperature attenuation under the ice cover.

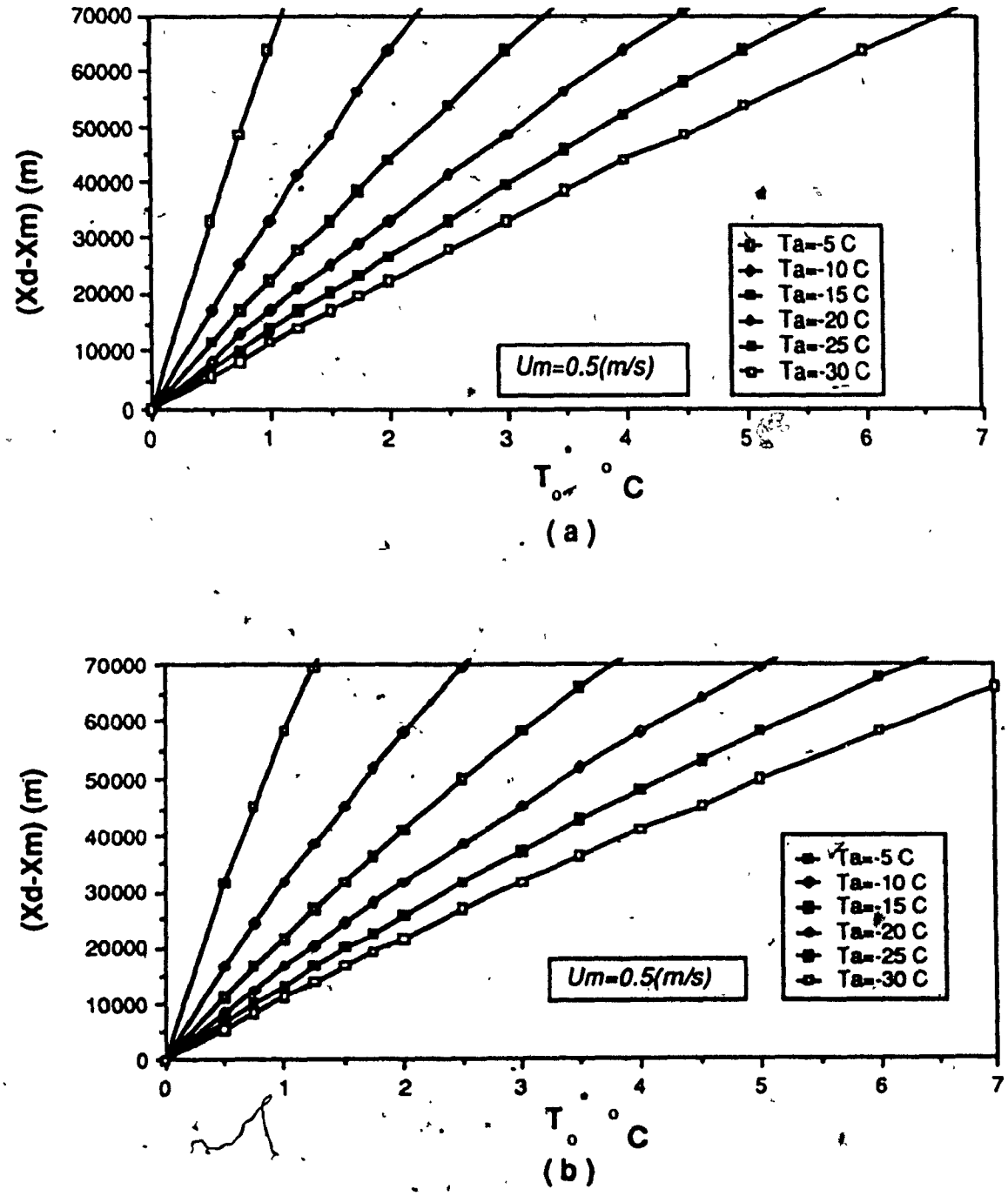

Fig: (3.4)Downstream locations of the ice cover edge;

a) Uniform flow; b) Divergent flow.

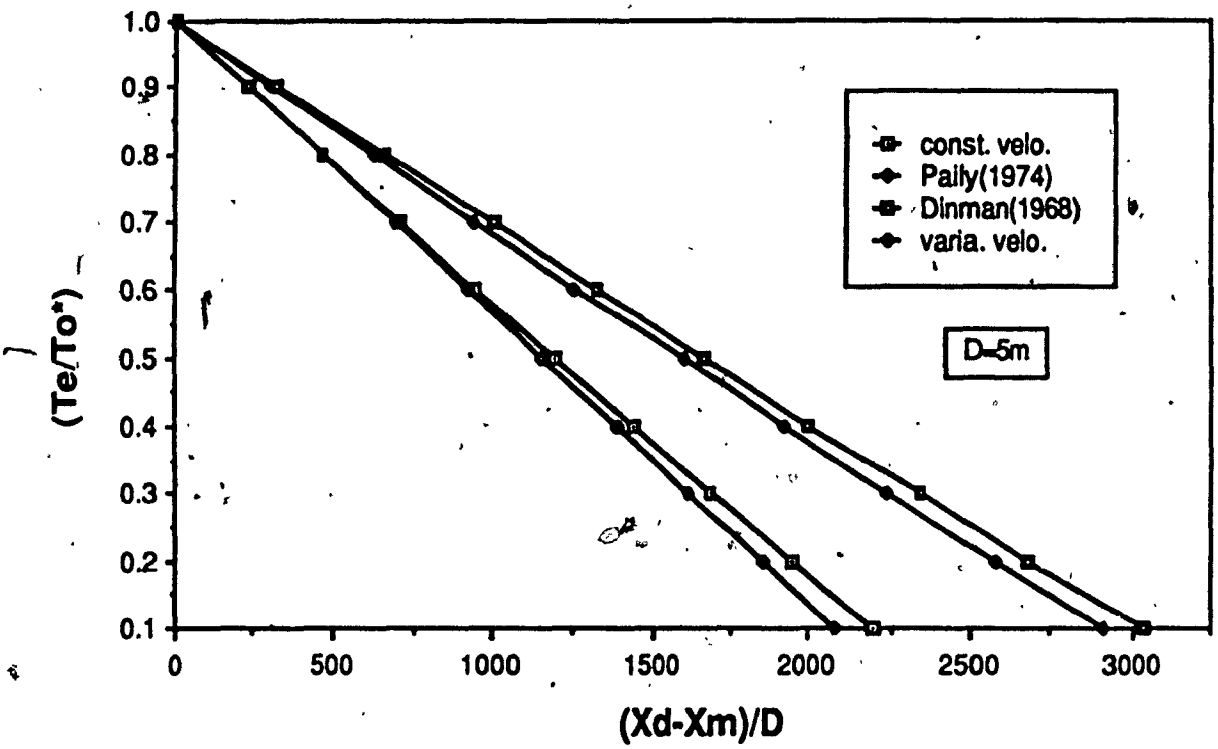

Fig: (3.5) Comparison of obtained solutions with previous works.

3.3 Ice Cover Suppression Criterion:

The discharge of a tributary thermal effluent into a cold water river usually results in a substantial loss of heat to the ice cover, leading to a thermal stratification in the receiving water body beneath the ice cover. The portion of heat which is not transfered to the atmosphere causes the local melting of the ice cover. A definition sketch for the upstream and downstream ice edge locations is shown in Fig. (3.1 a-b). The suppression of the ice cover is established by evaluating, separately, the locations of the upstream and the downstream ice edge based on the 0 °C isotherm criterion. The criterion for ice cover suppression is then fixed according to the ratio R of the distance from a datum X_o, of the upstream ice cover edge location, to the downstream ice edge . The ice cover is suppressed if, $R \leq 1$, that is:

$$R = \frac{x_u - x_o}{x_d - x_o} \leq 1 \qquad (3.17)$$

where: x_u : the upstream ice cover edge location

x_d : the downstream ice cover edge location

x_o : the datum point on the ice cover reach upstream of the thermal discharge section different from x_u.

However, in order to express R in terms of the heat balance equations, the following manipulation is introduced:

$$R = \frac{(x_u - x_o)}{(x_d - x_o)} = \frac{(x_m - x_o)}{(x_d - x_o)} + \frac{(x_u - x_m)}{(x_d - x_o)} \qquad (3.18)$$

where x_m is the location of the point of thermal discharge. Similarly, the right hand side terms of equation (3.18) may be expressed by:

$$\frac{(x_d - x_o)}{(x_m - x_o)} = \frac{(x_d - x_m)}{(x_m - x_o)} + \frac{(x_m - x_o)}{(x_m - x_o)} = \frac{(x_d - x_m)}{(x_m - x_o)} + 1.0 \qquad (3.19)$$

$$\frac{(x_d - x_o)}{(x_u - x_m)} = \frac{(x_d - x_m)}{(x_u - x_m)} + \frac{(x_m - x_o)}{(x_u - x_m)}$$

Each of the above terms is then replaced by its corresponding analytical expression as developed earlier, resulting in an expression of R in terms of the hydrodynamic and thermodynamic variables.

3.4 Discussion of the Formulations:

Figure (3.4 a-b) shows the location of the downstream edge of the ice cover (X_d-X_m) as a function of the initial mixing water temperature T_o^* for various air temperatures. The water depth was taken as 5m with an initial water velocity of 0.5m/sec. The linearity of the curves is peculiar to low air and mixing water temperatures. For different air temperatures there exists a certain value T_o^* at which the curves begin to behave non-linearly. This indicates that at low air temperatures, the effect of the mixing temperature is reduced and the advance of the ice cover edge is attenuated. The downstream distance to the ice cover edge (X_d-X_m) increases with the air or effluent water temperature.

Although the values of (X_d-X_m) shown in Fig. (3.4 b), for non-uniform flow, are lower

than those calculated under constant velocity conditions Fig. (3.4 a), the curve characteristics remain unchanged. However, it is noted that the upstream ice edge distance (X_u-X_m) from the point of thermal discharge is essentially a function of the apparent dispersion coefficient, and of the initial mixing water temperature T_o^*; and since the effect of the velocity was negligible, the formulation of the upstream distance to the ice edge (X_u-X_m) was not changed.

The suppression of the ice cover determined by the ratio R is presented in Fig.(3.6 a-b), which shows the effect of the receiving stream velocity on the ice cover, outlining the various conditions for ice cover suppression. In addition, the linear behaviour of the curves, at low air and initial mixing temperatures, implies that at higher values of T_o^*, the effect of the freezing air temperatures T_a is diminished. Ice cover suppression for uniform flow is also presented in Fig. (3.7 a-b), in terms of initial water mixing temperature for two air temperatures of -5°C and -15°C.

For the case of non-uniform flow Fig.(3.6b), the suppression of the ice cover is determined by evaluating the ratio R, taking into account the velocity variations. The effect of variability in the flow velocity is shown to be significant at lower air temperatures. Furthermore, in both cases, there exists a value T_o^*, at which, for different air temperatures, the ice cover would be suppressed. For the calculation presented in Fig. (3.6 a-b), the water depth was taken as 5m.

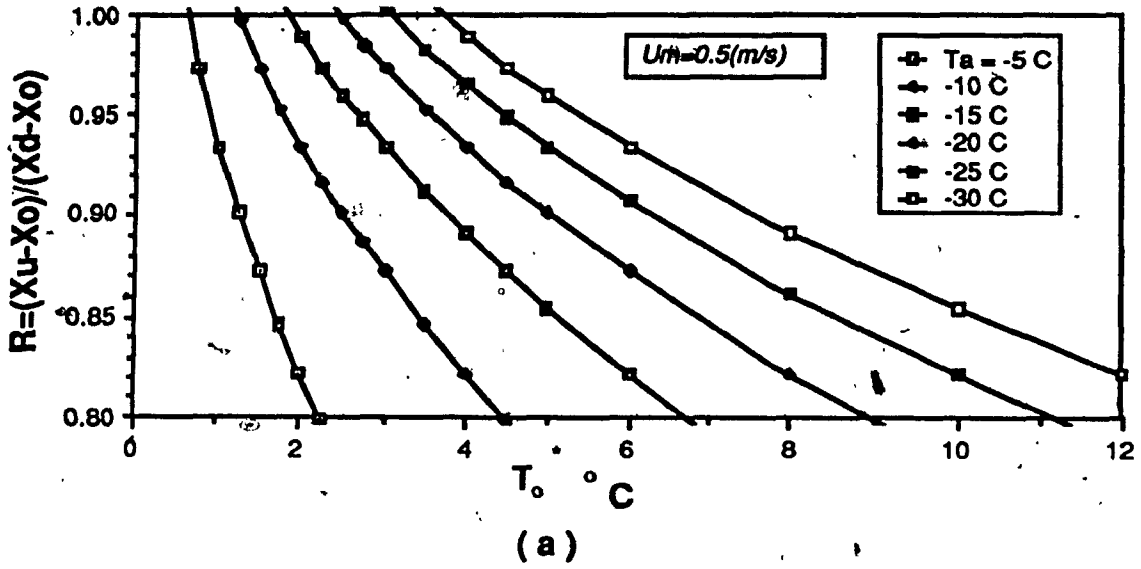

(a)

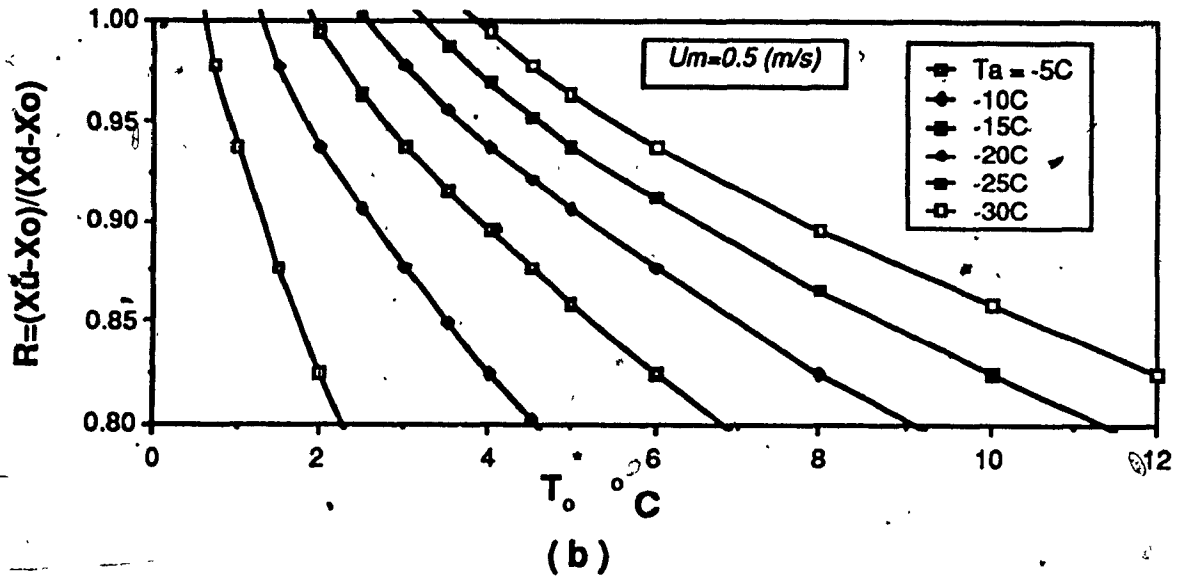

(b)

Fig. (3.6) Suppression of the ice cover:

a) Uniform flow; b) Divergent flow.

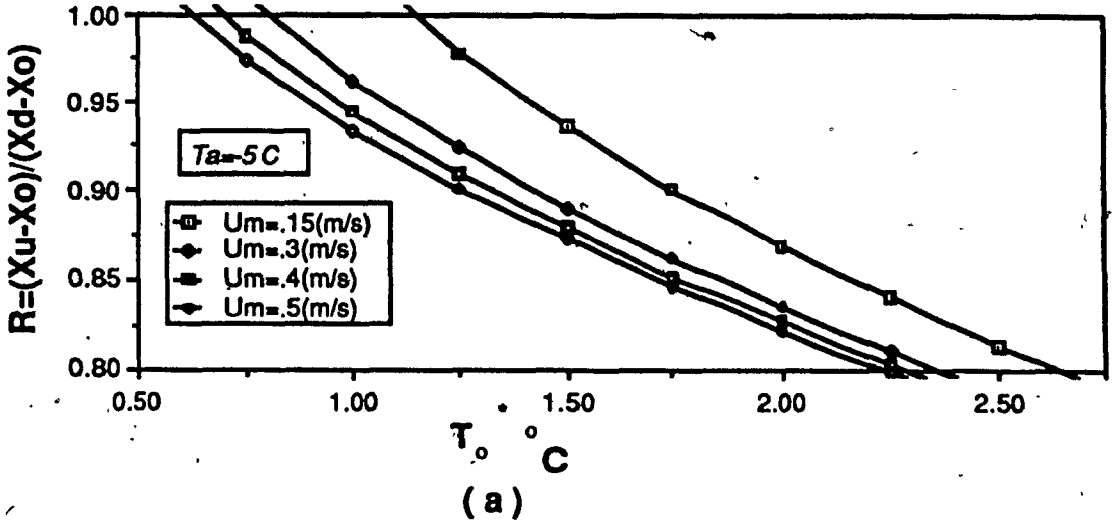

(a)

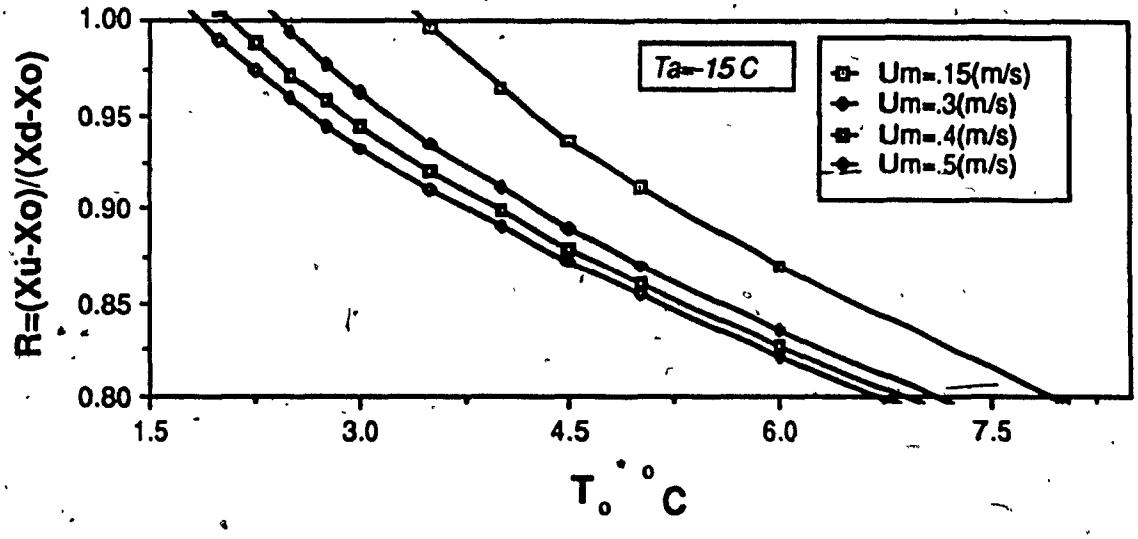

(b)

Fig. (3.7) Suppression of the ice cover for uniform flow:

a) T_a=-5 °C; b) T_a=-15 °C

Field Measurement:

In the winter of 1982/83, Hydro-Québec (Canada) carried out an observation and data collection campaign designed to study ice problems at the proposed Archipel Hydroelectric power plant at the Lachine Rapids on the St. Lawrence River[42]. Fig. (3.8) depicts the location of the observation sites on the St. Lawrence, in the vicinity of the city of Montreal. In this stretch of river, three distinct zones were observed . The first zone is located upstream of Lake St. Louis , with an average flow of 8400 m^3/s, and characterized by a stable ice cover. The extent of the stable ice cover in this zone varies significantly from year to year. The second zone covers the Lachine Rapids and remains completely ice free, except for a few areas near the shore. The third zone extends over Beauharnois canal with a relatively higher water temperature.

The main objectives of the campaign were: (1) the determination of the periods of formation of active frazil and its characteristics, (2) the observation of ice cover formation by analyzing photographs and charts of the ice sheet in the regime concerned, and (3) the measurement of local water temperature and velocity.The climatological factors were monitored at the Dorval Airport meteorological station.

For the purposes of this study, the ice cover maps, the water temperature, flow velocity and climatological factors were considered. Visual observations and aerial photographs were gathered to draw complete ice maps from the Cornwall Rapids to the Jacques Cartier Bridge. Measurement of the water temperature was made possible with the use of a floating helicopter. This survey consisted of determining the flow velocity and variation of the water temperature at the surface (1m depth) at different observation sites. The observations were performed in the following fashion: In zones of low velocity, the helicopter was able to settle on the water and the temperature was obtained at 1m depth. Once the velocity of the water became excessive, the measurements were taken from the air, again at a 1m depth. The thermometer used was "Dean

Engineering Associate" with a precision of 1/100 °C.

Thermal stratification at the entrance of Lake St. Louis in the zones of low velocity was noticed on March 5, 1983. A few temperature readings were taken beneath the ice cover on March 4 and 8, 1983; these varied between 0.09 to 0.32 °C. In addition, temperature measurements along the transversal sections of the flow were repeated 7 times in the same manner. The velocity of flow plays an important part in the thermal heat exchange at the water-air interface. It is therefore useful to measure both the velocity and temperature of the water at the same site. A series of flow velocities measured at various depths was collected at several observation sites. The velocity was measured using a *moulinet a coupoles*. Different stations were used to evaluate the velocity profile at 1m depth, as well as the transversal velocity profile.

High water velocities and perturbations produced by the ice were the major causes of difficulties encountered during the measurement of the water temperature. Therefore, in order to collect accurate temperature readings, the temperatures were measured regularly behind a wooden shield.

The presence of active frazil tended to falsify the temperature readings. Therefore, a suitable non-adhesive material was chosen for the thermometer rod.

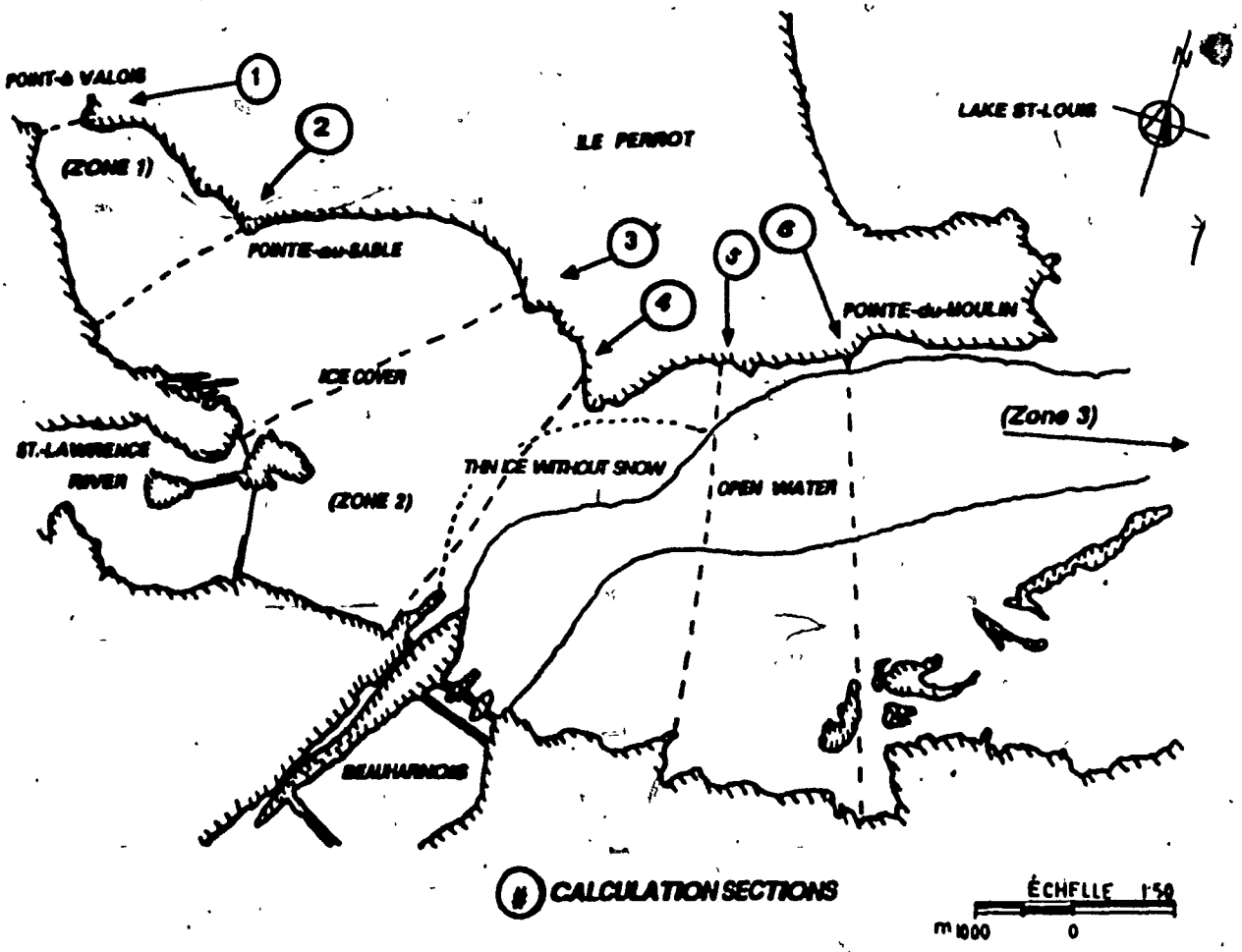

Fig. (3.8) Aerial map of the intersection of Beauharnois canal and Lake St-louis showing the positions of the upstream & downstream ice edges.

3.6 Field Data Comparison :

The site of the study centered on the intersection of the Beauharnois canal, the Vaudreuil channel, and the St-Lawrence River at the entrance of Lake St-Louis. A typical situation of upstream and downstream edges of the ice cover is shown in Fig. (3.8). The water depth was determined from topographic and bathymetric maps, along different sections between Pointe-A-Valois and the Beauharnois canal. The discharge rates for the three tributaries were recorded at various sites. Table [3.2] summarizes the discharges measured at various dates. Initial water mixing temperatures were recorded immediately downstream of the Beauharnois power plant, with a range varying from 0.03°C on the 14th of February, to 1.29°C on March 9th.

Two methods of calculation were carried out to check the validity of the formulation, and to test the derived equations against field data. At first, zero degree of thermal mixing was considered by assuming T_o^* equal to the effluent temperature. In the second instance, full mixing was considered according to equation (3.6). Both methods achieved a good agreement with observations. However, the second yielded smaller values for the location of the downstream ice edge due to the effect of the relatively cold water of the Vaudreuil channel. For example, on March 8, 1983, the following data were recorded: T_a=-1.9 °C, T_1=0.419 °C, and T_2=0.93 °C. The first method yields (X_d-X_m)=216.86 Km, (X_u-X_m)=1099.85 m, and R=0.642, while the second gives T_o^*=0.835 °C by equation (3.6), (X_d-X_m)=183.8 Km, (X_u-X_m)=973.6 m, and the ratio R is equal to 0.686. Both calculations indicate suppression of the ice cover. The same procedure was also used for the data from February 15, 17, March 4, 8 and 9, 1983, and was

in agreement with the observed conditions. It has been suggested from the calculations that the thermal effluent with a higher temperature does not fully mix unless the velocity of the receiving stream is high enough to suppress the ice cover in the receiving stream . The calculation results are shown in Fig.(3.9) through (3.12).

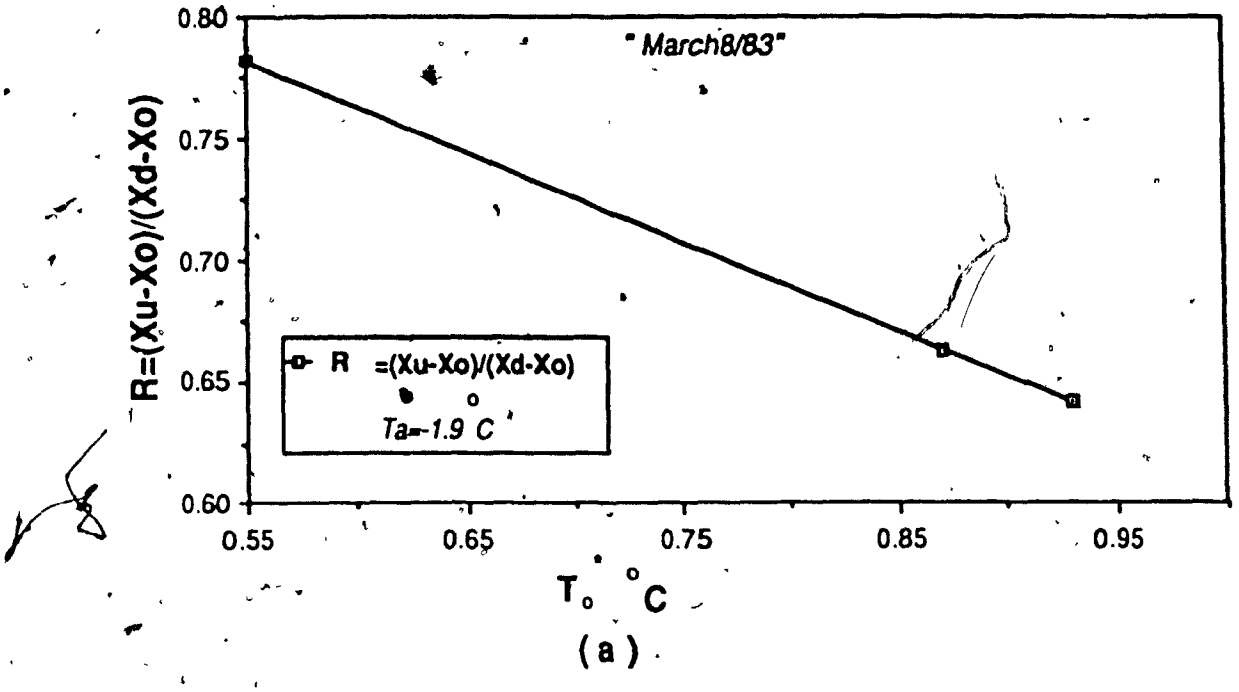

(a)

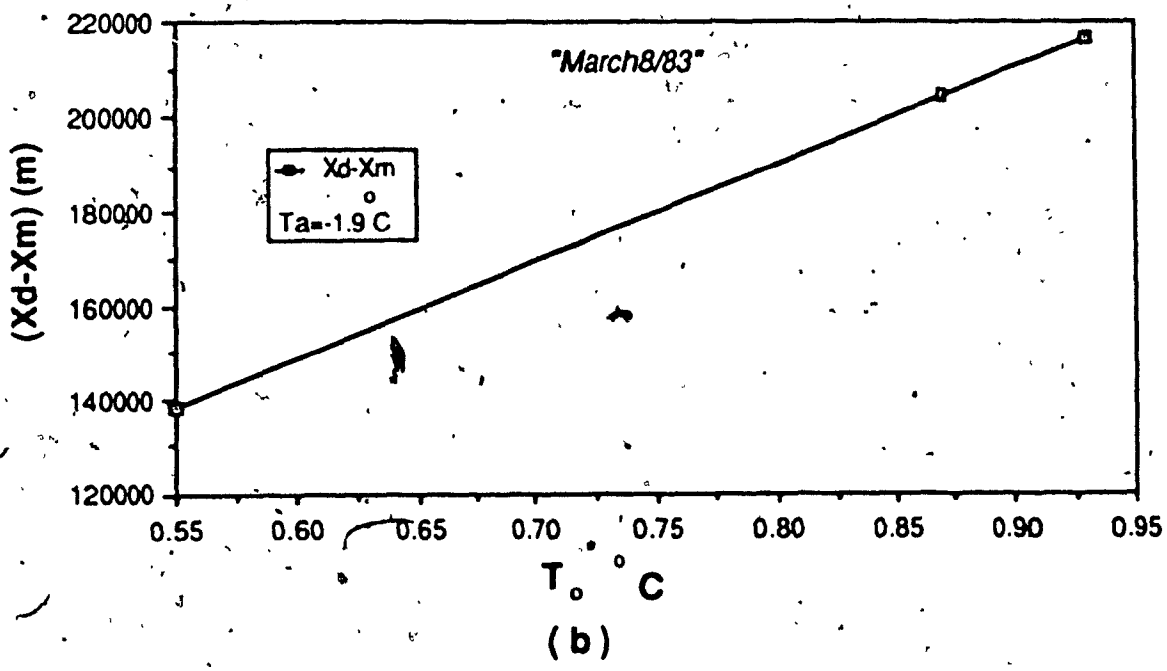

(b)

Fig. (3.9) Calculated ice conditions:

a) Suppression ratio; b) Downstream ice edge location.

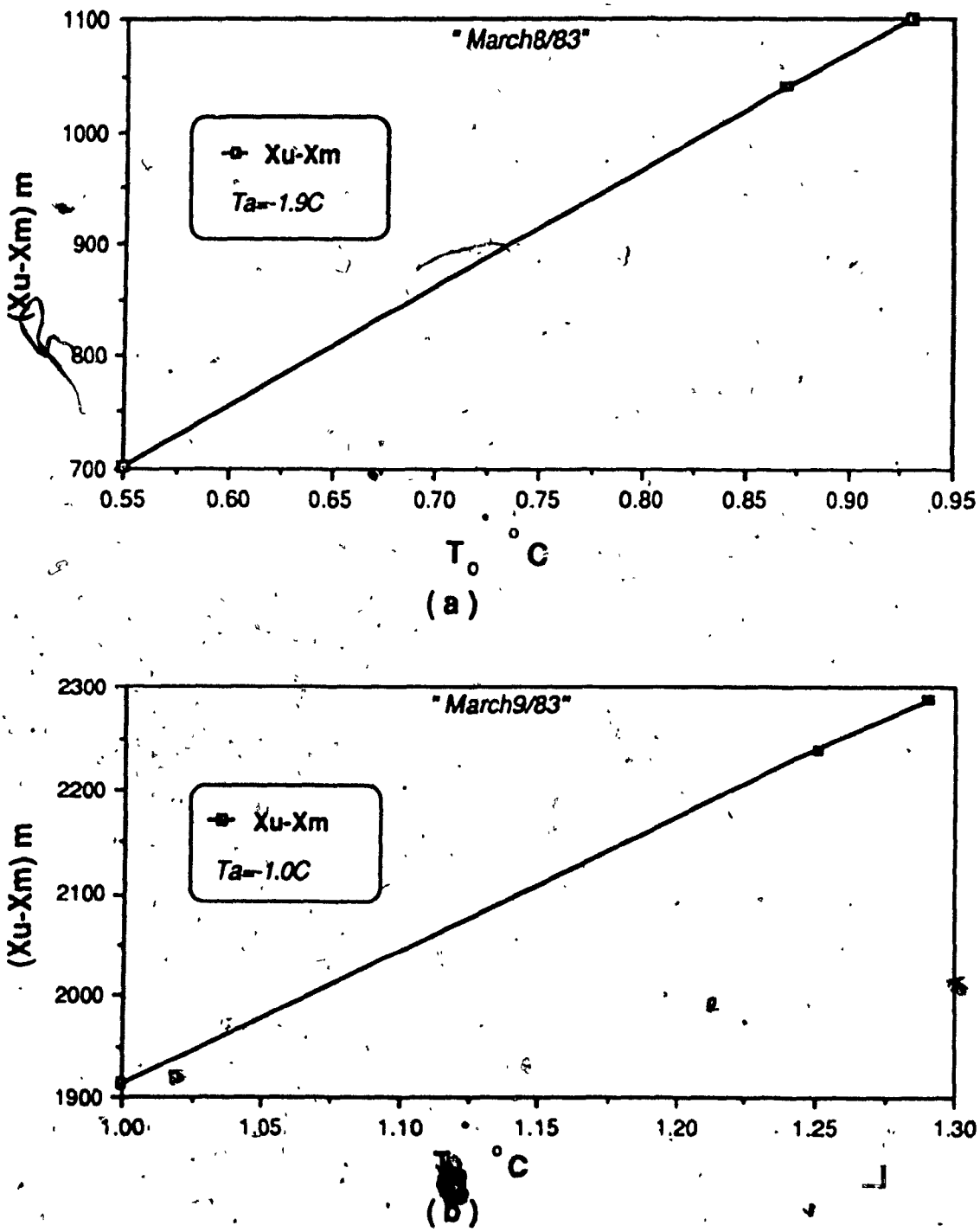

Fig. (3.10) Upstream ice cover edge locations for: a) March 8,1983; b) March 9,1983.

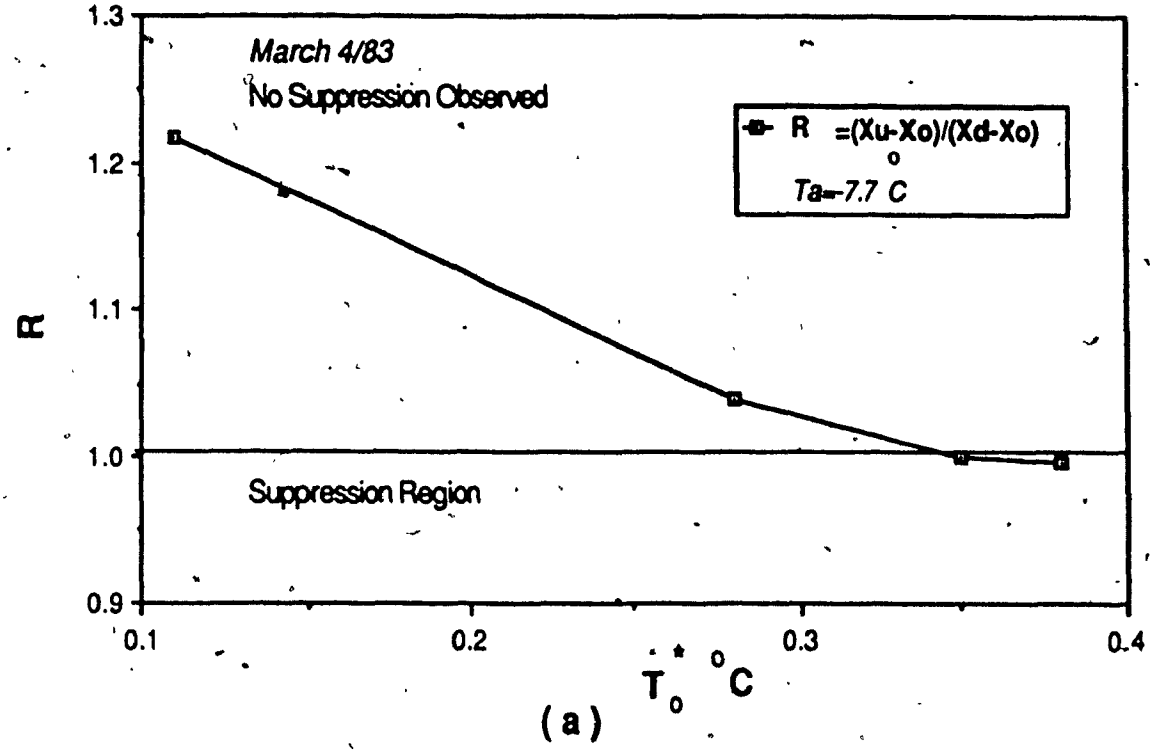

(a)

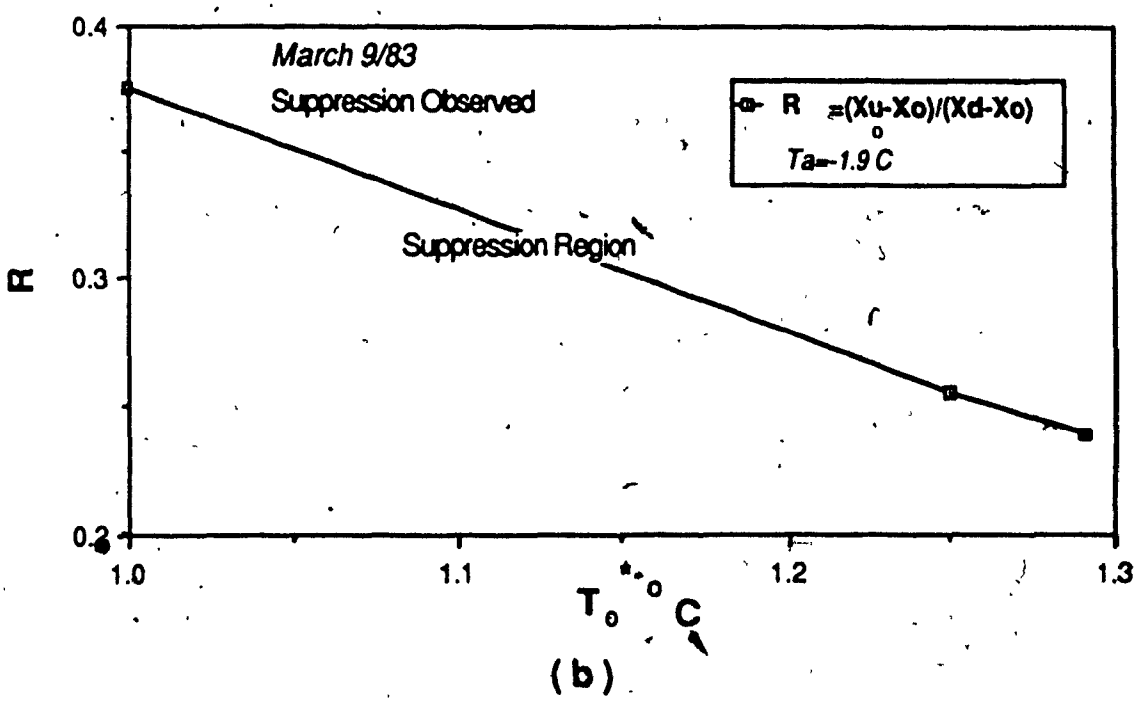

(b)

Fig. (3.11) Conditions of ice cover suppression for: a) March 4,1983; b)March 9,1983.

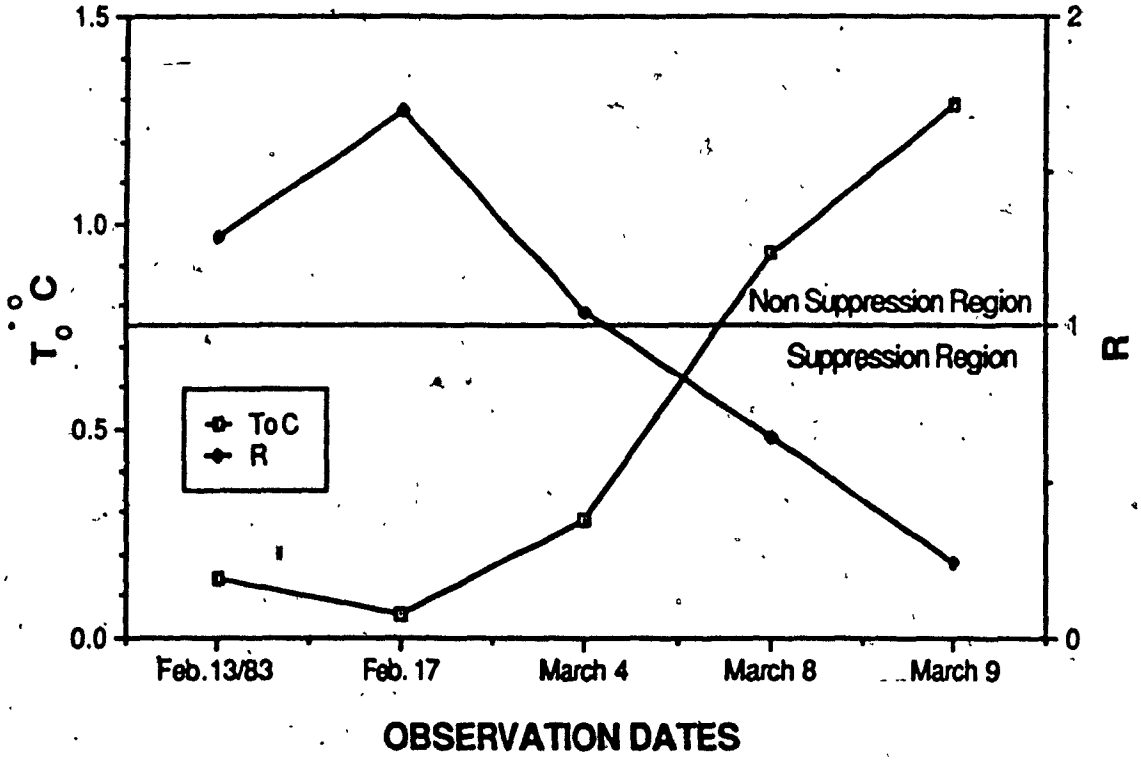

Fig. (3.12) Interrelation between the suppression ratio R and T_o^* for various observation dates.

CHAPTER IV

SOLUTION BY PERTURBATION TECHNIQUES

Many of the problems facing engineers involve such difficulties as nonlinear governing equations, variable coefficients, and nonlinear boundary conditions at complex (known or unknown) boundaries that preclude solving them exactly. Consequently, solutions are approximated using analytical" and/or" numerical techniques.

Foremost among the analytical techniques are the methods of perturbation (asymptotic expansions in terms of a small or a large parameter or coordinate). According to these perturbation techniques the solution is represented by the first few terms of a perturbation expansion, usually the first two. Although these perturbation expansions may be divergent, they can be more useful for a qualitative, as well as a quantitative, representation of the solution, than expansions that are uniformly and absolutely convergent. It is the rule, rather than the exception, that the straightforward expansions in powers of a parameter have limited regions of validity, and break down in certain regions, called regions of nonuniformity. To render these expansions uniformly valid; several investigators have developed a number of techniques in which some are radically different, while others are slightly different interpretations of the same basic idea.

In this chapter, the perturbation method was applied based on the WKB approximation and the Liouville-Green transformation. In this manner, it is possible to investigate the effect of the flow velocity variability, in addition to the effect of the longitudinal diffusion, on the ice cover suppression. A general form solution for the one dimensional quasi-linear energy equation with variable flow velocity is obtained.

4.1 One Dimensional Quasi-Linear Equation:

In this section, a general solution of the quasi-linear equation with linearized heat loss term Eq.(2.3) is presented. The initial mixed temperature was taken according to Eq. (3.6). The boundary condition is given by $T=T_o^*$, at $x=x_m$. At a certain distance downstream of the point of discharge, the initial mixing water temperature T_o^* will reach the ambient river temperature T_1, under the influence of climatological factors. This distance is dependent on the meteorological factors, especially the air temperature, and on the thermal effluent discharge T_2.

Using the same assumptions mentioned in chapter-II, and by considering each term as daily averaged values, Eq. (2.3) becomes;

$$u(x)\frac{\partial T}{\partial x} - E_x\frac{\partial^2 T}{\partial x^2} + \frac{h_{wa}}{\rho C_p D}(T - T_a) = 0 \qquad (4.1)$$

Equation (4.1), which is a quasi-linear partial differential equation, can be solved to predict the thermal response of heated streams, with the initial boundary conditions mentioned earlier. Assuming,

$$K = \frac{h_{wa}}{\rho C_p D}$$

Taking, $\theta = K(T-T_a)$, and differentiating T, and θ with respect to x gives:

$$\frac{1}{K}\theta' = \frac{dT}{dx}$$

$$\frac{1}{K}\theta'' = \frac{d^2T}{dx^2} \qquad (4.2)$$

substituting (4.2) into eq.(4.1) yields,

$$\theta'' - \frac{u}{E}\theta' - \frac{K}{E}\theta = 0 \qquad (4.3)$$

The solution of this homogeneous second-order differential equation containing slowly varying coefficient, which involves the use of the Liouville-Green transformation, is:

$$\theta(x) = p(x)\, w(x) \qquad (4.4)$$

where p and w are chosen so that Eq. (4.3) is transformed into an equation whose dominant part has constant coefficients. It follows from Eq. (4.4) that:

$$\begin{aligned} \theta' &= p'w + pw' \quad \text{and,} \\ \theta'' &= p''w + 2p'w' + pw'' \end{aligned} \qquad (4.5)$$

Substituting for θ, θ' and θ'' in Eq.(4.3) leads to

$$p''w + 2p'w' + pw'' - \frac{u}{E}p'w - \frac{u}{E}pw' - \frac{k}{E}pw = 0 \qquad (4.6)$$

Forcing the coefficients of w' to be zero gives:

$$2p'w' - \frac{u}{E}pw' = 0 \qquad (4.7)$$

and Eq. (4.6) is reduced to;

$$w'' + \left[\frac{p''}{p} - \frac{u}{E}\frac{p'}{p} - \frac{k}{E}\right]w = 0 \qquad (4.8)$$

Equation (4.7) can be solved by separation of variables, which upon integration gives:

$$p = \exp\left[\int \frac{u}{2E}\,dx\right] \tag{4.9}$$

Now,

$$p' = \frac{u}{2E}\exp\left[\int \frac{u}{2E}\,dx\right]$$

and,

$$p'' = \frac{u^2}{4E^2} + \frac{u'}{2E} \quad \exp\left[\int \frac{u}{2E}\,dx\right]$$

Substituting p' and p'' in equation (4.8) yields:

$$\frac{d^2w}{dx^2} + \left[\frac{u'}{2E} - \frac{u^2}{4E^2} - \frac{K}{E}\right] w = 0 \tag{4.10}$$

assume $X = x/\lambda$;

where, λ is a large variable compared with x. Expressing the equation in terms of the new variable X, yields:

$$\frac{dw}{dx} = \frac{dw}{dX}\cdot\frac{dX}{dx} = \frac{dw}{dX}\cdot\frac{1}{\lambda} \tag{4.11}$$

and substituting into equation (4.10), yields:

$$\frac{d^2w}{dX^2} + \lambda^2 q(X)\, w = 0 \tag{4.12}$$

where:

$$q(X) = \frac{u'}{2E} - \frac{u^2}{4E^2} - \frac{k}{E}$$

This is a differential equation with a large non-dimensional parameter; therefore the WKB approximation can be applied.

4.1.1 The WKB Approximation:

Assuming that q(X) in Eq. (4.12) is differentiable, and dividing by λ^2 yeilds:

$$\frac{1}{\lambda^2} w'' + q(X)\, w = 0 \qquad (4.13)$$

Letting $\lambda \to \infty$ in (4.13) leads to q(X)=0; this yields the trivial solution. Therefore, the solution cannot be determined by seeking an approximation in the form,

$$w(X) = w_0(X) + \frac{1}{\lambda} w_1(X) + \frac{1}{\lambda^2} w_2(X) + \ldots \qquad (4.14)$$

hence instead of seeking straightforward expansion in inverse powers of λ, an expansion in the following form will be applied,

$$w = e^{\lambda G(X,\lambda)} \qquad (4.15)$$

where G has a straightforward expansion in inverse power of λ, in the following form:

$$G(X\lambda) = G_0(X) + \frac{1}{\lambda} G_1(X) + \frac{1}{\lambda^2} G_2(X) + \ldots \qquad (4.16)$$

Differentiating Eq. (4.15) twice yields:

$$w' = \lambda G' e^{\lambda G} \quad ; \text{and} \quad w'' = (\lambda^2 G'^2 + \lambda G'') e^{\lambda G}$$

Substituting for w, w' and w'' in the linear equation (4.12), we transform it into the following nonlinear equation :

$$\left(G_0 + \frac{1}{\lambda}G_1 + \frac{1}{\lambda^2}G_2 + \ldots\right)^2 + q + \frac{1}{\lambda}\left(G_0' + \frac{1}{\lambda}G_1' + \frac{1}{\lambda^2}G_2' + \ldots\right) = 0 \quad (4.17)$$

Expanding and re-arranging the terms Eq. (4.17) yields:

$$G_0^2 + \frac{2}{\lambda}G_0 G_1 + q + \frac{1}{\lambda}G_0' + \ldots = 0 \quad (4.18)$$

Equating the coefficients of λ^0 and λ^{-1} to zero, we obtain,

$$G_0^2 + q = 0 \quad (4.19)$$

$$G_0' + 2G_0 G_1 = 0 \quad (4.20)$$

It follows from Eq. (4.19) that,

$$G_0^2 = -q$$

so that,

$$G_0 = \begin{cases} \pm i\sqrt{q} & \text{if } q > 0 \\ \pm\sqrt{-q} & \text{if } q < 0 \end{cases} \quad (4.21)$$

Then,

$$G_0 = \begin{cases} \pm i\int\sqrt{q}\,dX & \text{if } q > 0 \\ \pm\int\sqrt{-q}\,dX & \text{if } q < 0 \end{cases} \quad (4.22)$$

To solve, Eq. (4.20) we first divide it by $2G_0$, and obtain;

$$\frac{1}{2}\frac{G_0'}{G_0} + G_1 = 0 \quad (4.23)$$

which, upon integration gives;

$$G_1 + \frac{1}{2}\ln G_0 = 0 \quad (4.24)$$

The constant of integration is not needed as it becomes clear below. Hence,

$$G_1 = -1n\sqrt{G_0} \qquad (4.25)$$

Substituting for G_0 and G_1 in Eq. (4.16) gives

$$G = \pm i \int \sqrt{q}\, dX - \frac{1}{\lambda}\left[\ln\sqrt{\pm i} + \ln^4 \sqrt{q}\right] + \ldots \qquad q>0 \qquad (4.26)$$

and

$$G = \pm \int \sqrt{-q}\, dX - \frac{1}{\lambda}\left[\ln\sqrt{\pm 1} + \ln^4 \sqrt{q}\right] + \ldots \qquad q<0 \qquad (4.27)$$

Since u is usually a small value, $u'/2E$ is also a very small value. Therefore, the combination $(-u^2/4E^2)$ and $(-K/E)$ will result in a negative value for q(x). Hence, only Eq. (4.27) will apply in the present work.

Substituting Eq. (4.27) into Eq. (4.15) we have:

$$w = \exp\left\{ \pm i\lambda \int \sqrt{q}\, dX - \left[\ln\sqrt{\pm i} + \ln^4 \sqrt{q} \right] + \ldots \right\}$$

or,

$$w = \frac{\exp\left[\pm i\lambda \int \sqrt{q}\, dX\right]}{\sqrt{\pm i}\sqrt[4]{q}} + \ldots \qquad (4.28)$$

Equation (4.28) provides two linearly independent approximate solutions of (4.15). Expressing the exponentials in terms of trigonometric functions, an approximation to the general solution of Eq. (4.15) can be written in the form:

$$w = \frac{c_1 \exp\left[\lambda \int \sqrt{-q}\, dX\right] + c_2 \exp\left[-\lambda \int \sqrt{-q}\, dX\right]}{\sqrt[4]{-q}} + \ldots \quad \text{for } q<0 \qquad (4.29)$$

where C_1 and C_2 are arbitrary constants.

Equation (4.29) is usually referred to as a WKB approximation after Wentzel, Karmers and Brillouion. However, note that Eq. (4.29) breaks down at, or near, the zeros of q(X). These zeros are called turning or transition points.

Rewriting Eq.(4.29) in terms of x gives:

$$W \approx \frac{c_1 \exp\left[\int \sqrt{-q}\, dx\right] + c_2 \exp\left[\int -\sqrt{-q}\, dx\right]}{\sqrt[4]{-q}} + \ldots \qquad q<0 \qquad (4.30)$$

Now substituting Eq. (4.30) in Eq. (4.4) to find the value of θ yields,

$$\theta \approx \frac{c_1 \exp\left[\int \sqrt{-q}\, dx\right] + c_2 \exp\left[-\int \sqrt{-q}\, dx\right]}{\sqrt[4]{-q}} \cdot \exp\left[\int \frac{u}{2E}\, dx\right] + \ldots \qquad q<0 \qquad (4.31)$$

Also we can find the value of θ for q>0 in the same way. By applying the boundary conditions, that is at $x \to \infty$, $\theta \Rightarrow 0$ or $T = T_a$

$\therefore c_1 = 0$, and θ can be evaluated for;

$$\theta = \frac{c_2 \exp\left[-\int \sqrt{-q}\, dx\right]}{\sqrt[4]{-q}} \cdot \exp\left[\int \frac{u}{2E}\, dx\right] \qquad (4.32)$$

Comparison of the above equation with previous works is presented in Fig. (4.1).

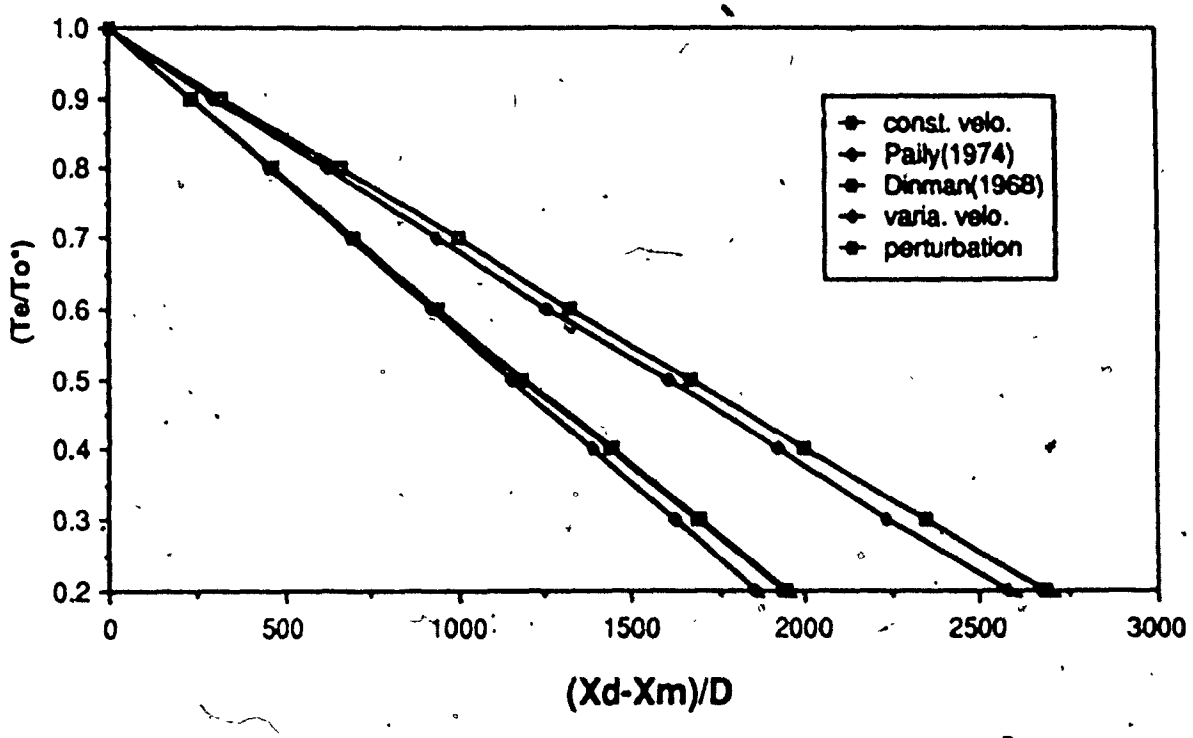

Fig. (4.1) Comparison of obtained solutions with previous works.

4.2 Uniform Flow case

This example demonstrates an evaluation for a uniform channel flow with constant flow velocity; it also helps to examine the validity of the general form solution for such flow conditions.

In this case, q(x) has a negative value. Therefore equation (4.29) should be applied, and the final form solution becomes;

$$\log_e\left[\frac{T-T_a}{T_o-T_a}\right] = -\left[\left(\frac{u^2}{4E^2}+\frac{K}{E}\right)^{\frac{1}{2}} - \frac{u}{2E}\right](x-x_m) \qquad (4.33)$$

From the above equation the location of the downstream ice cover edge, the 0 °C isotherm, becomes;

$$(x_d - x_m)_{T_e=0} = \frac{\log_e\left[\frac{T_e-T_a}{T_o-T_a}\right]}{-\left[\left(\frac{u^2}{4E^2}+\frac{K}{E}\right)^{\frac{1}{2}} - \frac{u}{2E}\right]} \qquad (4.34)$$

Equation (4.34) represents the movement of the downstream edge of the ice cover as a function of the initial mixing temperature T_o, and the air temperature T_a. This relation is shown in Fig. (4.2 b) for different initial mixing water and air temperatures. In this figure, the curves seem to have a non-linear behaviour at high air temperature, and to behave linearly at low air temperature. In fact, at low air temperatures, the water surface looses relatively more heat, and large part of the thermal input to the ice cover will be transferred to the atmosphere,

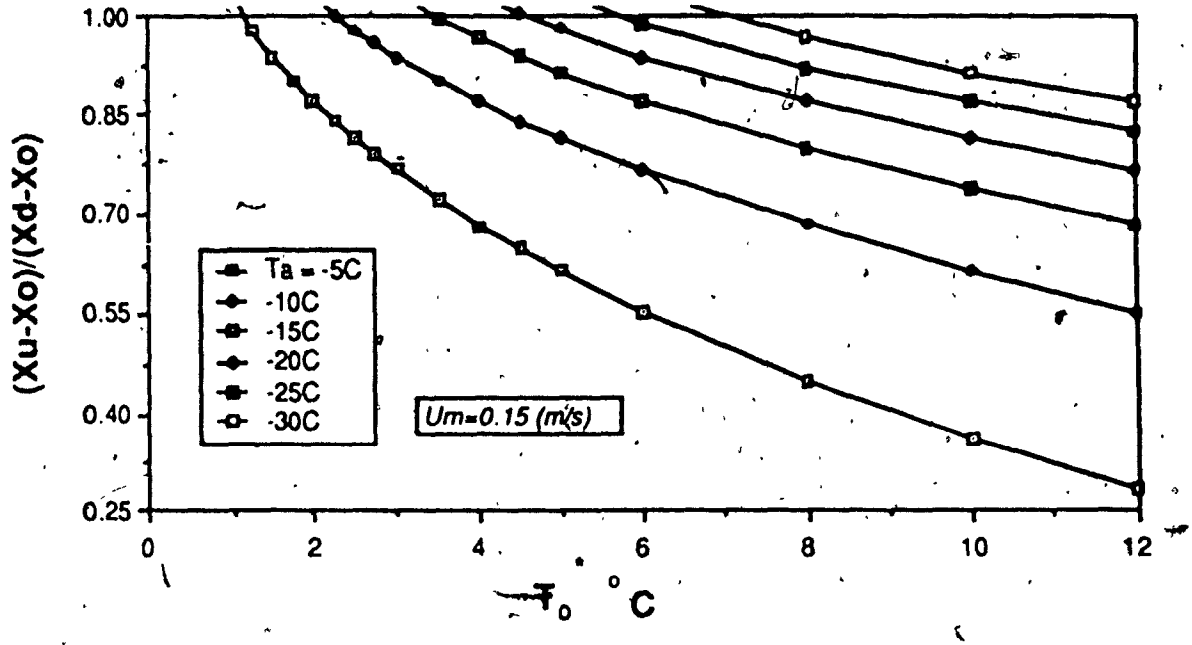

(a)

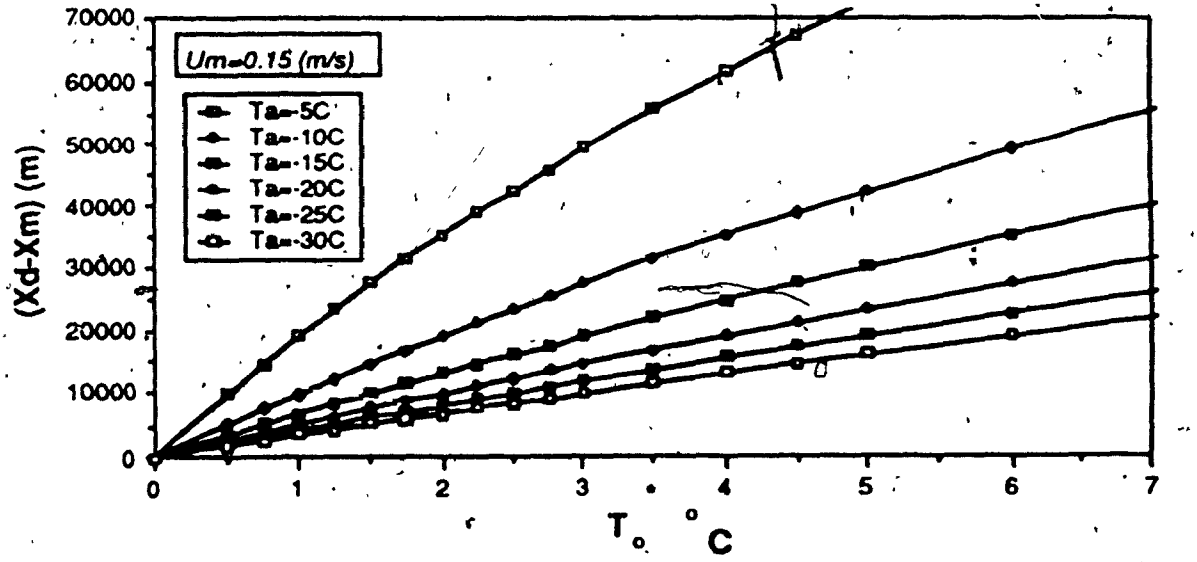

(b)

Fig. (4.2) Calculated ice conditions:

a) Suppression ratio; b) Downstream ice edge location.

thereby reducing the effect of the thermal effluent discharge, and resulting in slower advancement of the ice cover edge. On the other hand, at relatively high air temperature, the rate of heat transfer to the atmosphere is smaller, therefore keeping the heat input within the receiving water body, and causing a large downstream movement of the ice edge. The various conditions for the ice cover suppression are shown in Fig. (4.3 a).

By comparing the results obtained by this method with those obtained from equations (3.8, 3.16) for the same conditions, it is revealed that they agree at low initial water mixing temperatures, while at higher values of T_o^* and lower air temperatures, some discrepancy exists.

4.3 Divergent Flow Case:

The effect of the flow variability is examined through a divergent channel, where the flow velocity decreases along the longitudinal flow direction. The velocity is assumed to be represented by the following equation ;

$$u = K'(X - X_m) + u_m$$

where:

$$K' = \frac{-30}{\rho C_p D}$$

By applying the boundary conditions, the final solution yields:

$$\left[\frac{T-T_a}{T_o-T_a}\right]\frac{\left[\frac{\Delta}{2E}+\frac{u^2}{4E^2}\right]_{x=x_m}^{\frac{1}{4}}}{\left[\frac{\Delta}{2E}+\frac{u^2}{4E^2}\right]^{\frac{1}{4}}}$$

$$\frac{\exp\left\{\frac{1}{4EK}\left[u\sqrt{u^2+a^2}+a^2\log_e\left(\frac{u+\sqrt{u^2+a^2}}{a}\right)-u^2\right]\right\}=A}{\exp\left\{\frac{1}{4EK}\left[u\sqrt{u^2+a^2}+a^2\log_e\left(\frac{u+\sqrt{u^2+a^2}}{a}\right)-u^2\right]\right\}_{x=x_m}=B} \qquad (4.35)$$

where, $\Delta = (2K + K')$, $a^2 = 2E\Delta$

$u = u_m$ at $x = x_m$

$$A=\exp\frac{1}{4EK}\left[-K'(x-x_m)+u_m\sqrt{\left[-K'(x-x_m)+u_m\right]^2+2E(2K+K')}+\right.$$

$$\left.2E(2K+K').\log_e\left[\frac{\left[-K'(x-x_m)+u_m\right]+\sqrt{\left[-K'(x-x_m)+u_m\right]^2+2E(2K+K')}}{\sqrt{2E(2K+K')}}\right]-\right.$$

$$\left.\left[-K'(x-x_m)+u_m\right]^2\right. \qquad (4.36)$$

and

$$B = \exp\frac{1}{4EK}\left[u_m\sqrt{u_m^2+2E(2K+K')}+2E(2K+K')\right]$$

$$\log_e\frac{\left(u_m+\sqrt{u_m^2+2E(2K+K')}-u_m^2\right)}{\sqrt{2E(2K+K')}} \qquad (4.37)$$

Equation (4.35) shows the effect of the variation of the receiving stream velocity on the ice cover suppression. Since the flow velocity is an important factor in the mixing process of the thermal effluent discharge, and in heat transport, it is desirable to investigate its variability effect by the perturbation techniques. In this section, the suppression of the ice cover is determined by evaluating the ratio:

$$R = \frac{x_u - x_0}{x_d - x_0}$$

where x_u-x_0 is the distance from the upstream ice edge to the datum point x_0, and x_d-x_0 is the distance from the downstream ice edge to the same datum point. This has been done by taking into account the velocity variations and the longitudinal dispersion terms. In a divergent channel, and since the flow velocity decreases along the longitudinal direction, the ice cover is given the opportunity to be established. This implies that higher values of the initial water mixing temperature will be required to suppress the ice cover. Fig. (4.3a-d) shows that the effect of the variable velocity is significant on the movement of the downstream ice edge. Fig. (4.3a-d) represents the movement of the downstream ice cover edge, (x_d-x_m), as a function of the initial mixing water temperature T_o^* for different air temperatures. The flow characteristics are the same as in the previous example. Although the values (x_d-x_m) shown in Fig. (4.3a-d) are lower than those calculated in the previous case, the curve characteristics remain unchanged.

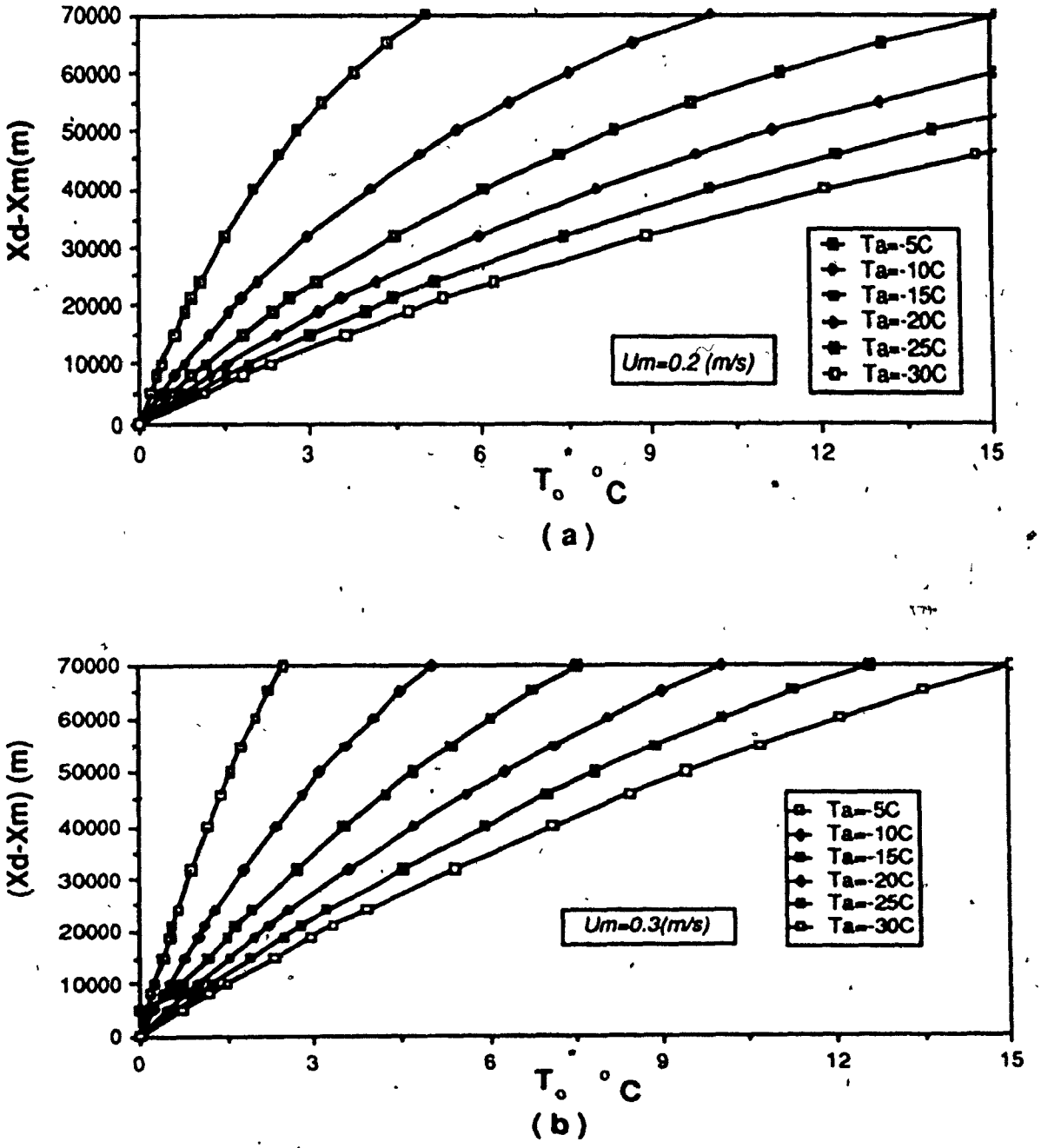

Fig. (4.3) Downstream location of the ice edge for a divergent channel with initial flow velocity of: a) u_m =0.2 m/sec; b) u_m=0.3 m/sec.

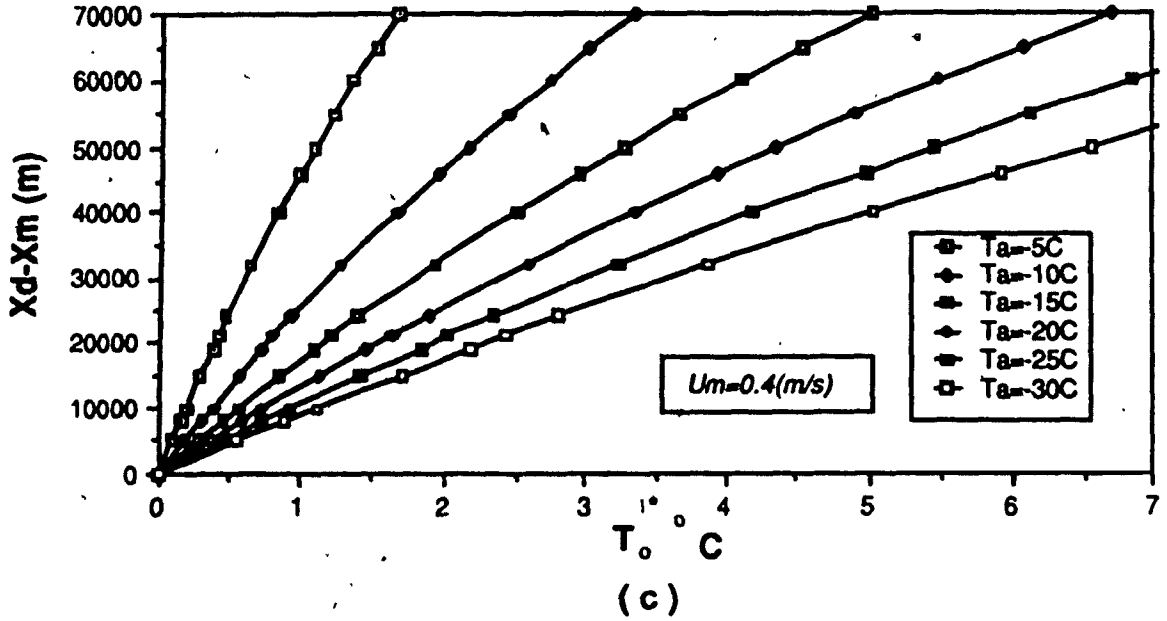

(c)

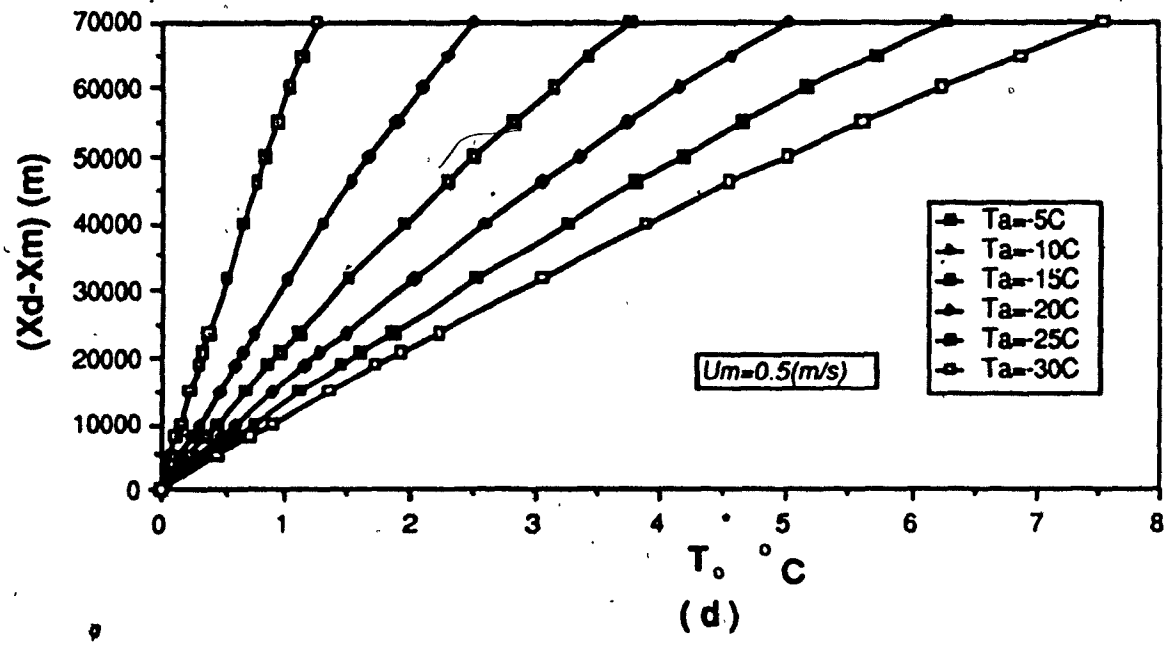

(d)

Fig. (4.3) Downstream location of the ice edge for a divergent channel with initial flow velocity

c) u_m=0.4 m/sec; d) u_m=0.5 m/sec.

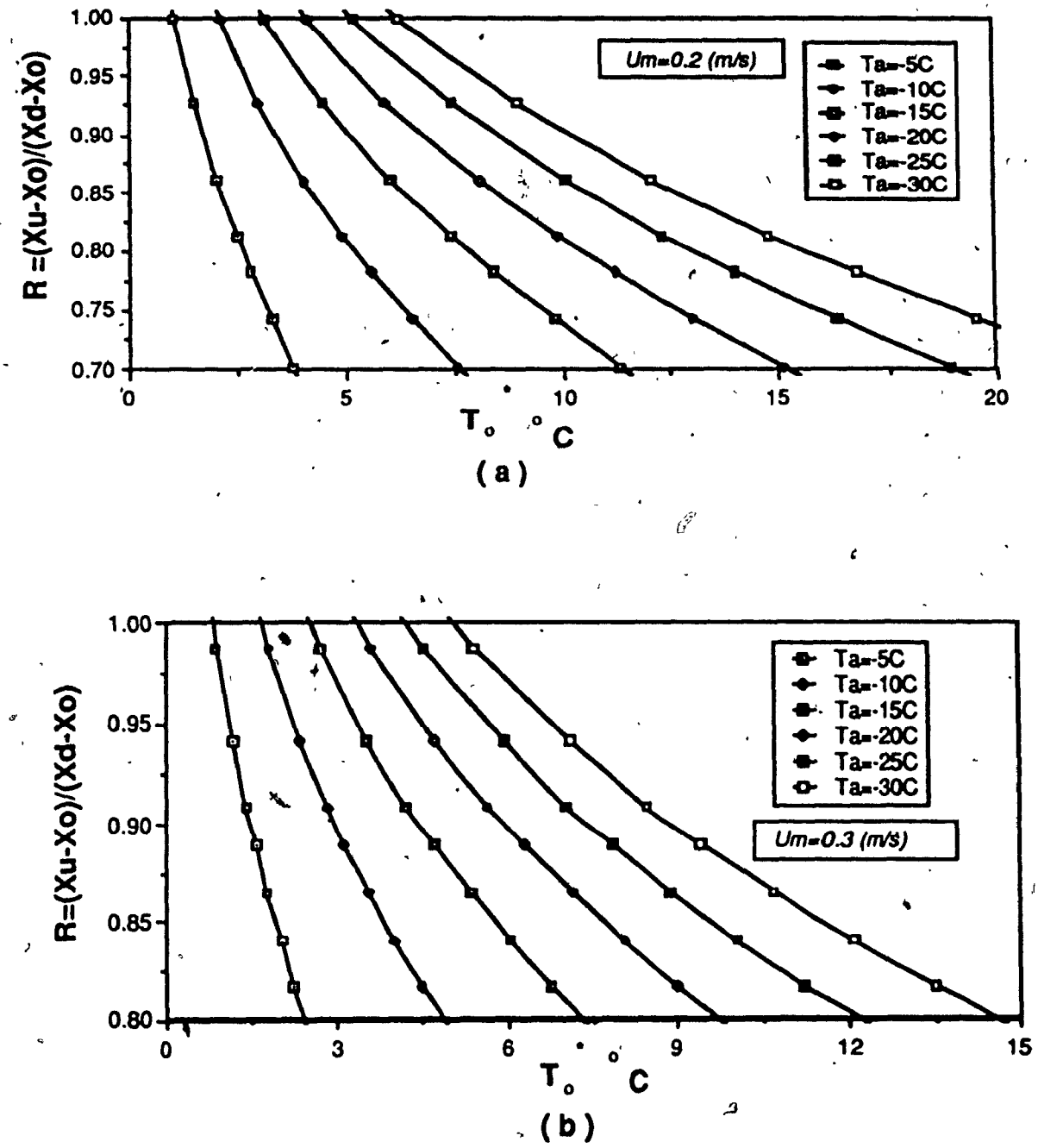

Fig. (4.4) Suppression of the ice cover for a divergent channel with initial flow velocity of:

a) u_m=0.2 m/sec; b) u_m=0.3 m/sec.

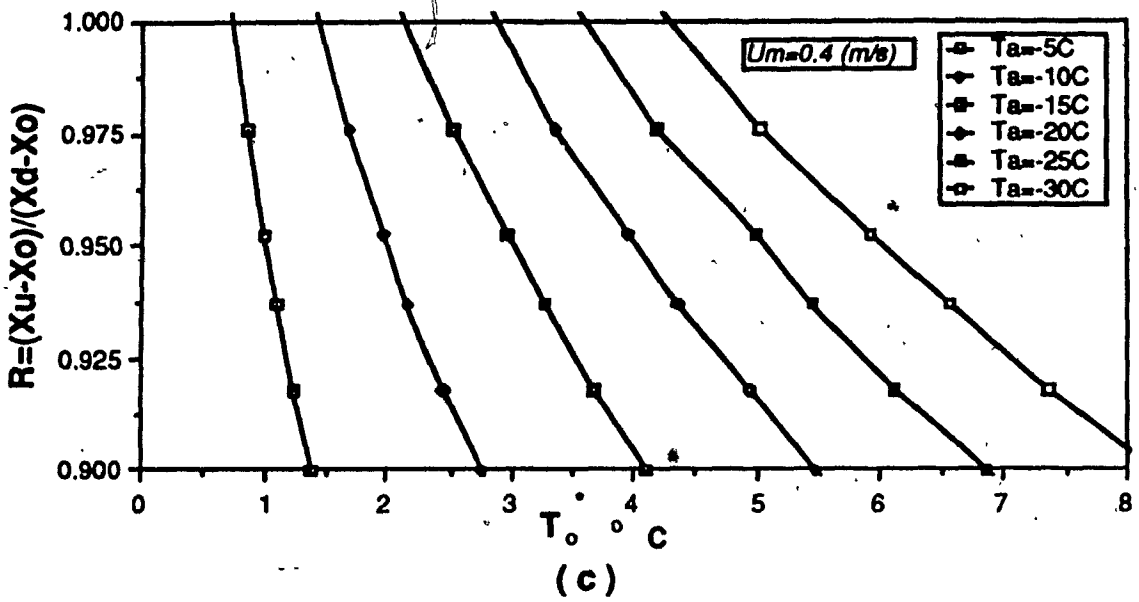

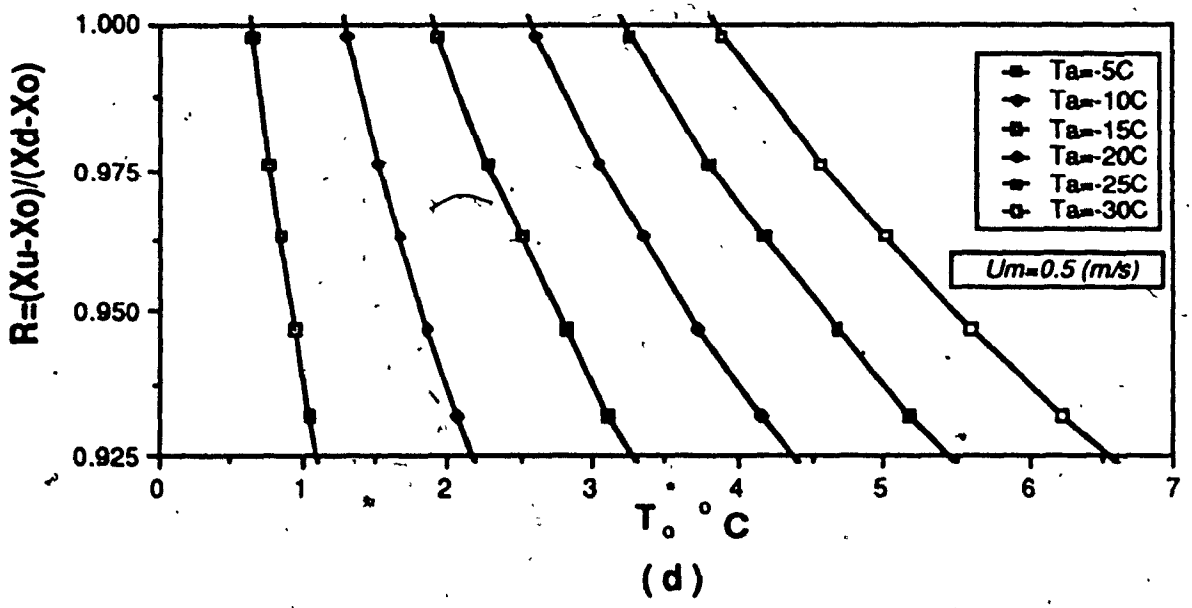

Fig. (4.4) Suppression of the ice cover for a divergent channel with initial flow velocity of:

c) u_m=0.4 m/sec; b) u_m=0.5 m/sec.

For example, for air temperature is -30 °C, and T_o^* =1.5 °C, the value of (x_d-x_m) will be 10 Km for u_m of 0.2 m/sec where the value of (x_d-x_m) is equal to 6 Km for a flow velocity of 0.3 m/sec, for the same initial water mixing temperature. The various conditions for the ice cover suppression are obtained from Fig. (4.4a-d). The above results are for the same conditions mentioned earlier.

4.3 Convergent Flow Case:

For a convergent channel, much lower values of the initial mixing temperature are required to suppress the ice cover under given meteorological conditions. This example evaluates the downstream distance to the ice cover edge (x_d-x_m). This value would progress faster downstream of the point of discharge, under the action of both the thermal effluent and the increase in the flow velocity. Assuming the velocity to be represented by $u= K' (X-X_m)+u_m$ with,

$$K' = \frac{30}{\rho C_p D} .$$

and after integrating and applying the boundary condition at $x = x_m$, $T = T_o^*$, and $u = u_m$ at $x = x_m$ the final solution yields:

$$\frac{T-T_a}{T_o^*-T_a} = \frac{\left[\frac{u^2}{4E^2}+\frac{(2K-K')}{2E}\right]_{x=x_m}^{\frac{1}{4}}}{\left[\frac{u^2}{4E^2}+\frac{(2K-K')}{2E}\right]^{\frac{1}{4}}}$$

$$\frac{\exp\left\{-\frac{1}{4EK'}\left[u\sqrt{u^2+b^2}+b^2\log_e\frac{(u+\sqrt{u^2+b^2})}{b}-u^2\right]\right\}}{\exp\left\{-\frac{1}{4EK'}\left[u\sqrt{u^2+b^2}+b^2\log_e\frac{(u+\sqrt{u^2+b^2})}{b}-u^2\right]\right\}_{x=x_m}} \qquad (438)$$

where, $\Delta' = 2K - K'$, $b^2 = 2E\Delta'$.

The velocity action on the ice cover suppression will increase with the velocity increase in the longitudinal direction, starting from the point of discharge in the downstream direction. Fig. (4.5a-b) shows the downstream distance to the ice cover edge (x_d-x_m), for initial flow velocity of 0.15, 0.3 m/sec.

From Fig. (4.6a-b) the ice cover suppression will be faster in a convergent channel than in a divergent one. For instance, from Fig. (4.6a-b), the ice cover suppression will occur at $T_o^* = 0.783$ °C for air temperature of -5 °C, and initial flow velocity of 0.3 m/sec, whereas under diverge channel condition, and some other parameters, the suppression will take place at $T_o^* = 1.09$ °C.

4.4 Flow Under Ice Cover Condition:

In this section, a general form solution to evaluate the water temperature attenuation under the ice cover into the downstream direction is developed. As is mentioned in chapter-II, the heat flux from ice-covered rivers can be expressed by $\Phi = \Phi_{wi} = h_{wi}(T-T_m)$. Substituting

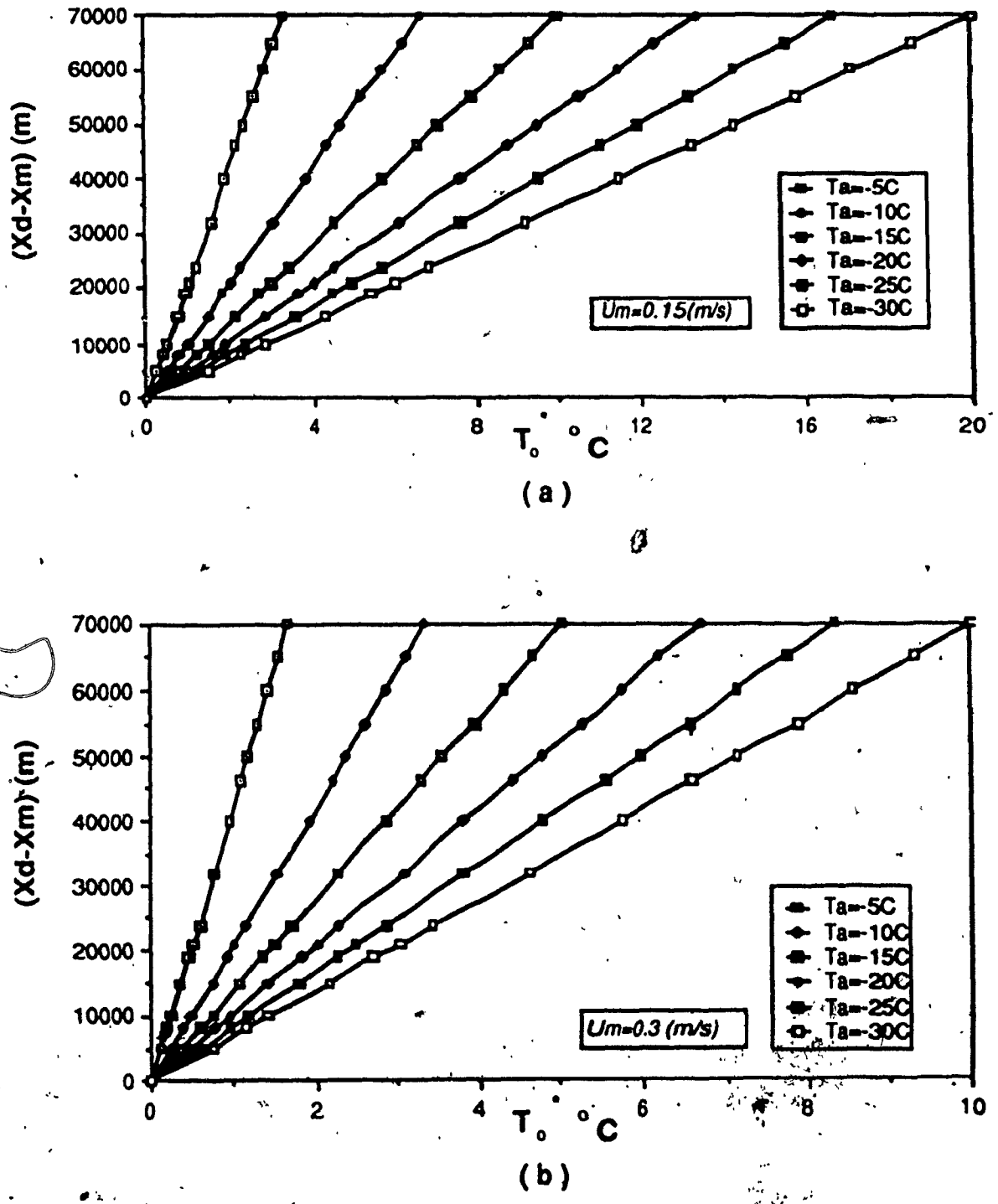

Fig. (4.5) Downstream location of the ice edge for a convergent channel with initial flow velocity of: a) u_m=0.15 m/sec; b)u_m=0.30m/sec.

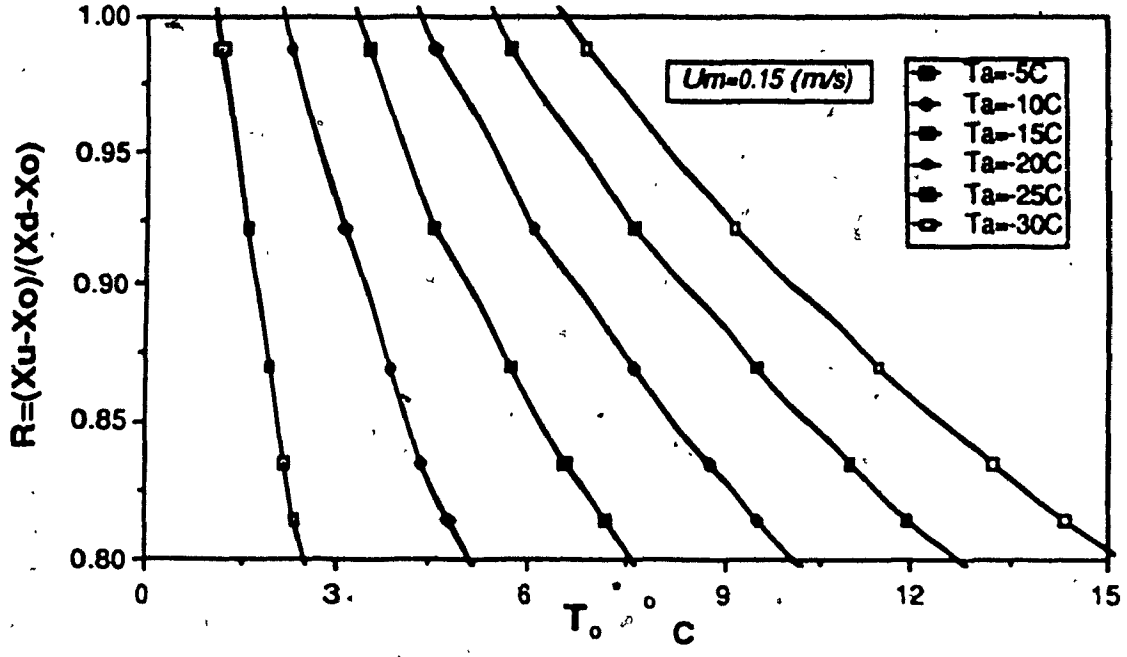

(a)

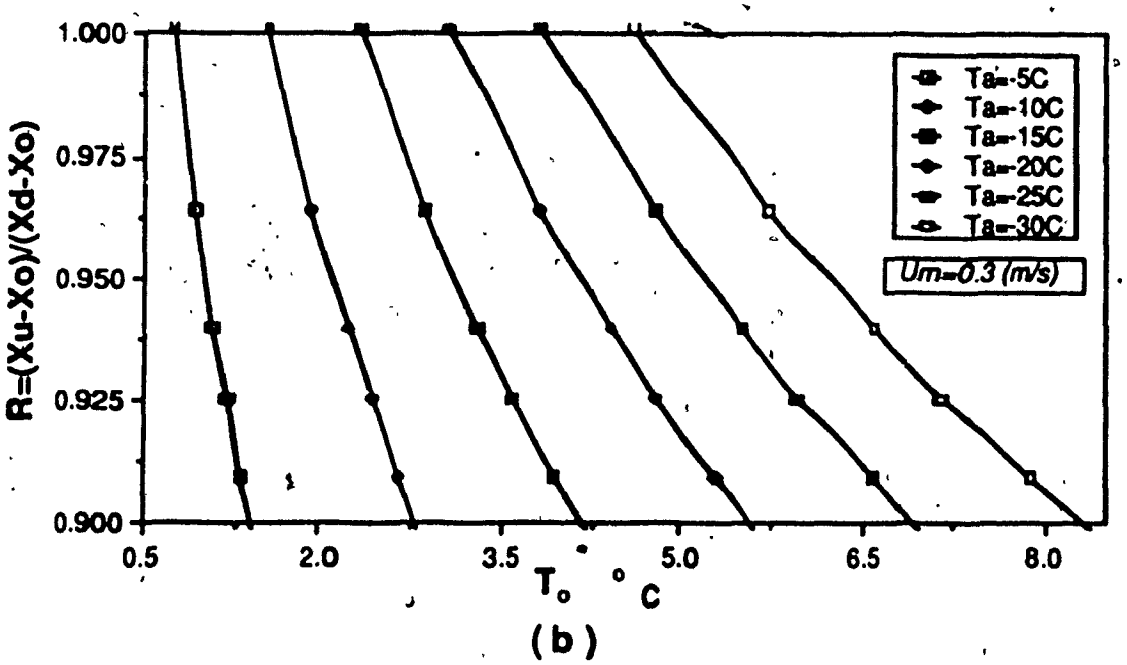

(b)

Fig. (4.6) Suppression of the ice cover for a convergent channel with initial flow velocity of:

a) u_m=0.15 m/sec; b) u_m=0.3 m/sec.

for Φ in equation (4.1) yields;

$$u(x)\frac{\partial T}{\partial x} - E_x\frac{\partial^2 T}{\partial x^2} + \frac{h_w}{\rho C_p D}(T - Tm) = 0 \qquad (4.39)$$

However, the heat transfer coefficient at the water-ice interface h_{wi} is a function of the velocity and is represented by the following Eq. after [37]:

$$h_{wi} = 1622\frac{u^{0.8}}{D^{0.2}},$$

assuming;

$$K = \frac{1622}{\rho C_p D},$$

equation (4.39) can be written as:

$$E\frac{\partial^2 T}{\partial x^2} - u\frac{\partial T}{\partial x} - u^{0.8}K(T - T_m) = 0 \qquad (4.40)$$

taking;

$$\theta = K(T - T_m)$$

Substituting into eq. (4.40) , and rearranging the terms yields:

$$\theta - \frac{u}{K}\theta'' - u^{0.8}\frac{K}{E}\theta = 0 \qquad (4.41)$$

This equation is a second-order differential and homogeneous equation, which could be solved by applying the Liouville-Green transformation and the WKB approximation. Therefore, by following the same steps as in the previous case, the final form solution is as follows:

$$\theta = \frac{C_1 \exp\left[\int \sqrt{-q}\, dx\right] + C_2 \exp\left[-\int \sqrt{-q}\, dx\right]}{\sqrt[4]{-q}} \cdot \exp\left[\int \frac{u}{2E} dx\right] \qquad (4.42)$$

where,

$$q(x) = \left[\frac{u'}{2E} - \frac{u^2}{4E^2} - u^{0.8}\frac{K}{E}\right]$$

Applying the boundary conditions at $x \to \infty$, $\theta \to 0$ or $T = T_m$, and $C_1 \to 0$ the general form solution will be:

$$\theta = \frac{C_2}{\sqrt[4]{-q}} \cdot \exp\left\{-\int\left(\sqrt{-q} - \frac{u}{2E}\right) dx\right\} \qquad (4.43)$$

Applying the following boundary condition at $x = x_o$, $T = T_o$, eq. (4.43) yields:

$$\frac{T - T_m}{T_o - T_m} = \exp\left\{-\left[\left(\frac{u^2}{4E^2} + u^{0.8}\frac{K}{E}\right)^{\frac{1}{2}} - \frac{u}{2E}\right](x - x_o)\right\} \qquad (4.44)$$

This equation represents the water temperature attenuation under the ice cover, and is represented in Fig. (4.7), for different initial flow velocity and depth.

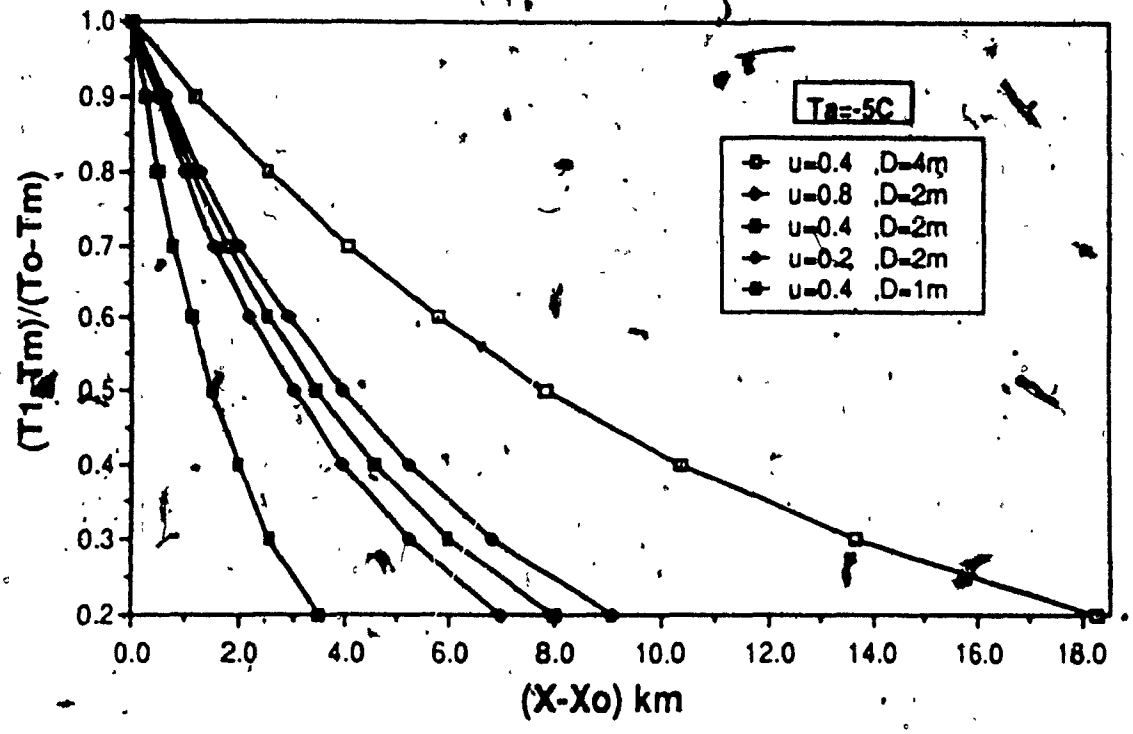

Fig. (4.7) Calculated water temperature attenuation under the ice cover..

CHAPTER V

FIELD COMPARISON FOR PERTUBATION SOLUTION

In order to check the validity of the present work, it is tested against field data. The same set of data that has been applied in the previous work will be used again to compare the results obtained by the perturbation method. Two methods of calculation are used. The first assumes the water temperature values, which are measured just in front of Beauharnois power plant, as the initial water mixing T_o^*. The second method assumes these values as the water temperature from the power plant itself, and by using equation (3.6). In what follows, we will demonstrate a sample of calculation for each case.

5.1 Sample (1), Case N0. (1)

On March 8, 1985, the air temperature Ta = - 1.9 °C three mixing water temperatures were measured, for which the values are:

T_o^* = 0.55 °C , 0.87 °C , 0.93 °C

The first step in calculation is to evaluate the value of downstream distance of the ice edge (x_d-x_m), which was found equal to 216.871 km according to Eq. (4.32). The second step is to evaluate the upstream distance to the ice edge, (x_u-x_m) from equation (3.12), and it is found to be (1099.84)m in the upstream direction. The model presented in eqs. (3.17-3.19) provides the conditions for the ice cover suppression. The ratio R, for T_a^* = 0.93, is R = 0.642 < 1,

indicating that the ice cover will be suppressed, which was the case for March 8, 1983. The same model was also used for the dates of Feb. 15, Feb. 17, March 4, and March 9 of 1983. (see Fig (5.1)).

Sample (2) Case No. (2)

In this case, the water temperature attenuation under the ice cover is calculated for the Vaudreuil channel and the St. Lawrence River to the intersection of the Beauharnois canal. The first step consists in evaluating the water temperature attenuation in the Vaudreuil channel starting from *Pointe-à-Valois*. This section has the following characteristics for March 8, 1983:

1- The initial water temperature T_0=0.05 °C

2-The average flow depth 4.8m

3-The average flow velocity u=0.0835 m/sec.

4-The flow rate Q=343.41 m^3/sec

Equation (4.44) is applied, and the ratio of T/T_0 for the section of 1635 m in length is equal to 0.908; which leads to T = 0.0454 °C. This value is taken as T_0 for the next section starting from *Point-aux-Sable*, where the flow characteristics for this section are:

1-u = 0.08 m/sec

2-D = 5.18 m

3-Q = 343.41 m^3/sec.

By applying equation (4.44) again, T/T_0 for section length of 2450 m is equal to 0.8767, which leads to a value for T = 0.098 °C. Again this value represents T_0 for the following section, which

starts from *Ile de Cascades*, and where the flow characteristics are:

1-u = 0.065 m/sec

2-D = 6.44 m

3-Q = 343.41 m^3/sec

Therefore the value of T/T_o is 0.9359.

At the intersection with the St. Lawrence River, and for a section length of 2850 m, the flow characteristics are as follows:

1-T_o = 0.58 °C

2-U = 0.57 m/sec

3-D=4.66 m

4-Q = 1937.1 m3/sec;

therefore T is equal to 0.487 °C, and the upstream water temperature can be evaluated as follows:

$$T_1 = \frac{Q\,T(\text{Vaudreuil}) + Q\,T(\text{St. Lawrence})}{Q(\text{Vaudreuil}) + Q(\text{St. Lawrence})} = 0.419\,^{\circ}C$$

Now, the initial mixing temperature at the mixing region in front of Beauharnois for March 8 will be calculated using equation (3.6) as follows:

$$T_o^{\cdot} = \frac{T_1 Q_1 + T_2 Q_2}{Q_1 + Q_2}$$

with; T_1 = 0.419 °C

T_2 = 0.93 °C

$T_o^{\cdot}$ = 0.835 °C

$Q_1 = 2280.51\ m^3/sec$

$Q_2 = 6941.9\ m^3/sec$

and the values of $(x_d-x_m) = 183.8$ km, $(x_u-x_m) = 973.6$ m and the ratio R is equal to 0.68649, indicating ice cover suppression.

By comparing both methods of calculation, it was found that the second method gives lower values for (x_d-x_m) and (x_u-x_m) because it takes into consideration the effect of the cold water from the upstream tributaries of the Vaudreuil channel and the St. Lawrence River. The same procedure was used for March 4 & 9, 1983 and the results are in Fig. (5.1) through Fig. (5.5).

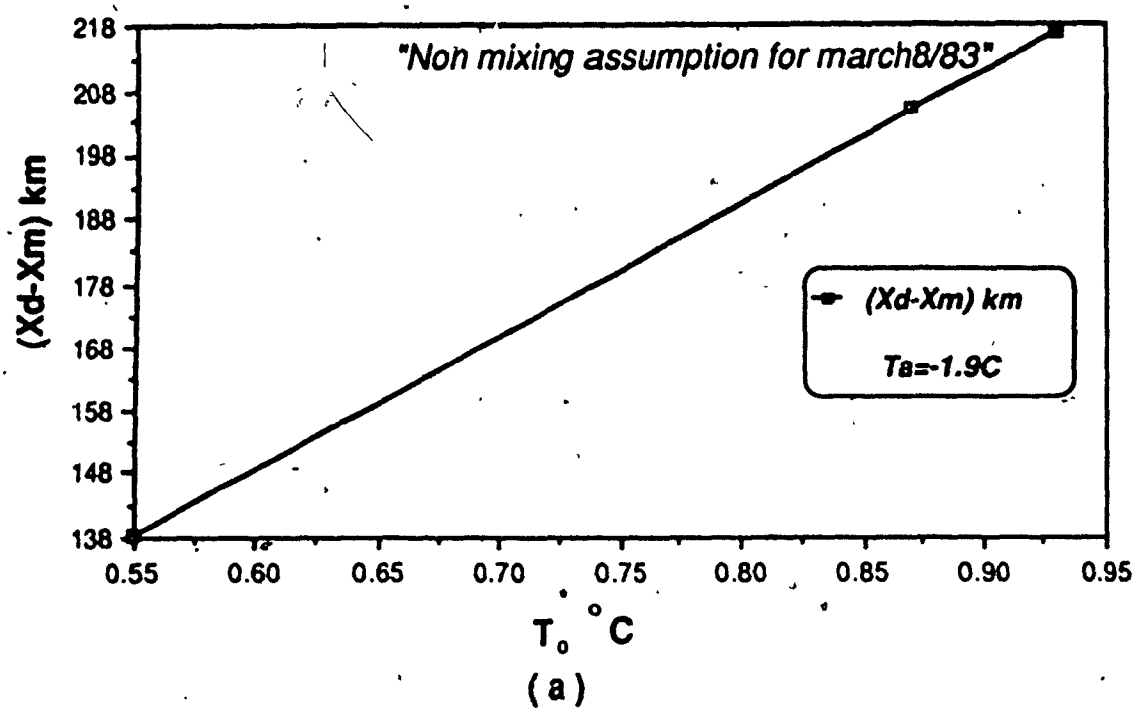

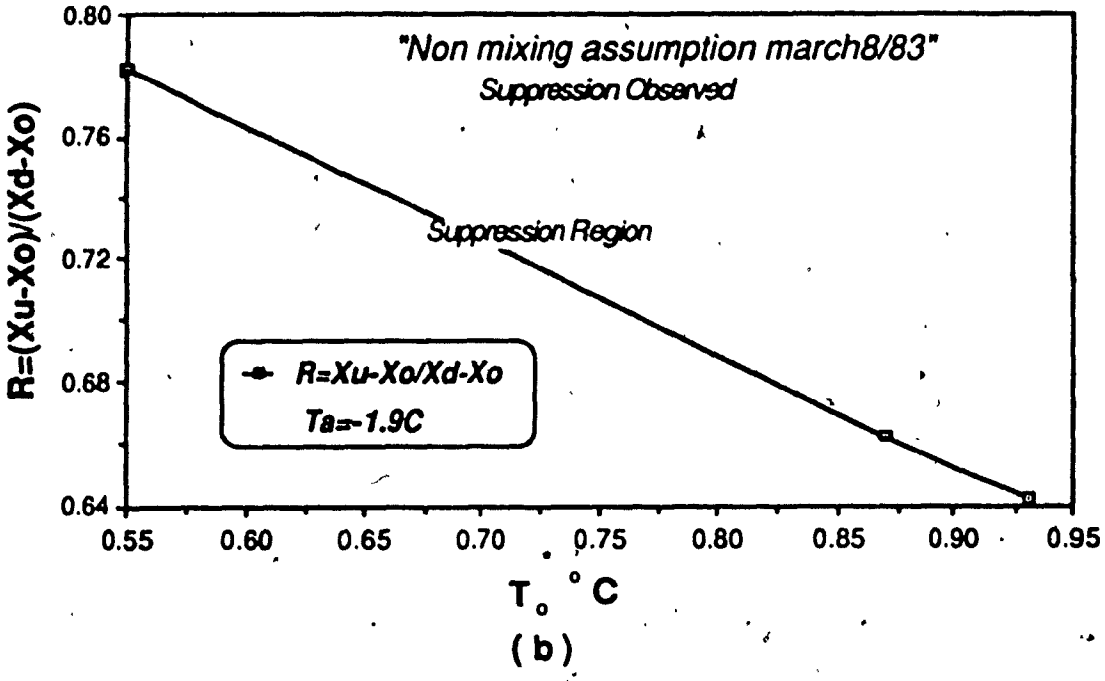

Fig. (5.1) Calculated ice conditions for non-mixing assumption for March 8,1983.

a) downstream ice edge; b) suppression ratio.

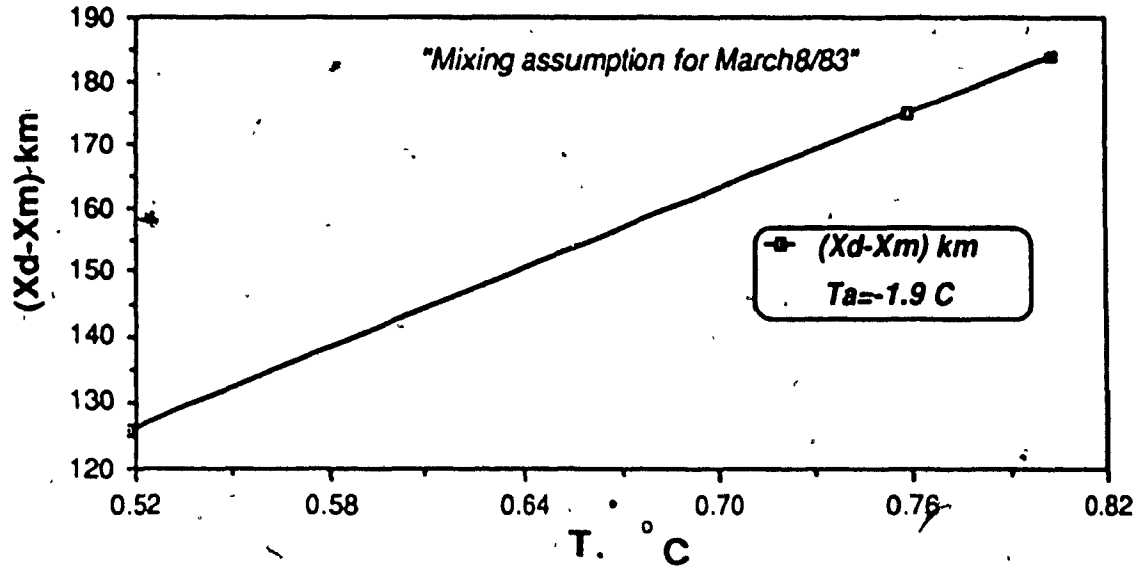

(a)

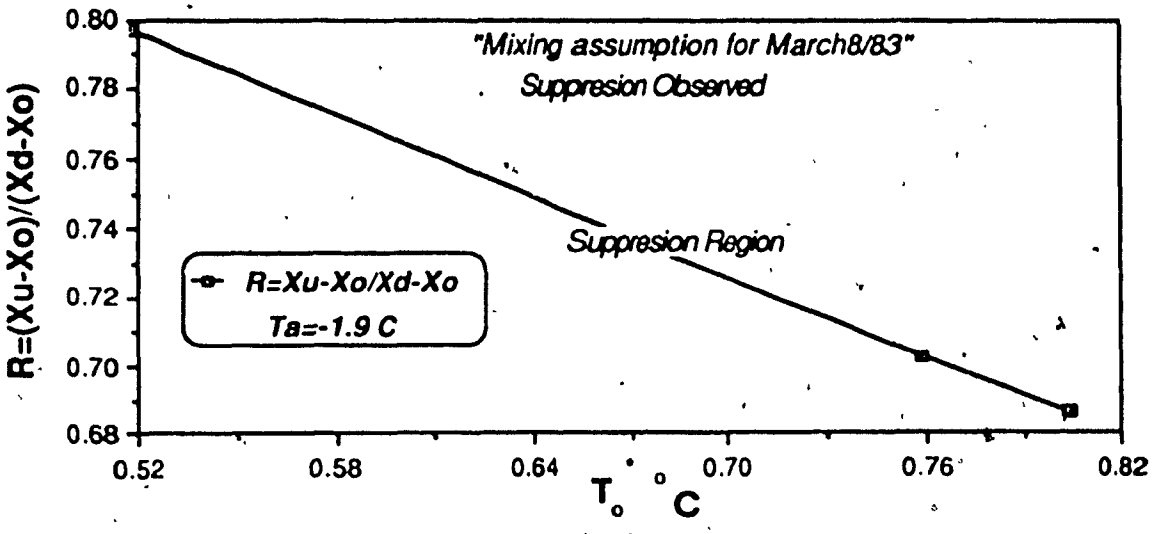

(b)

Fig. (5.2) Calculated ice cover conditions with mixing assumption for March 8,1983.

a) downstream ice edge; b) suppression ratio.

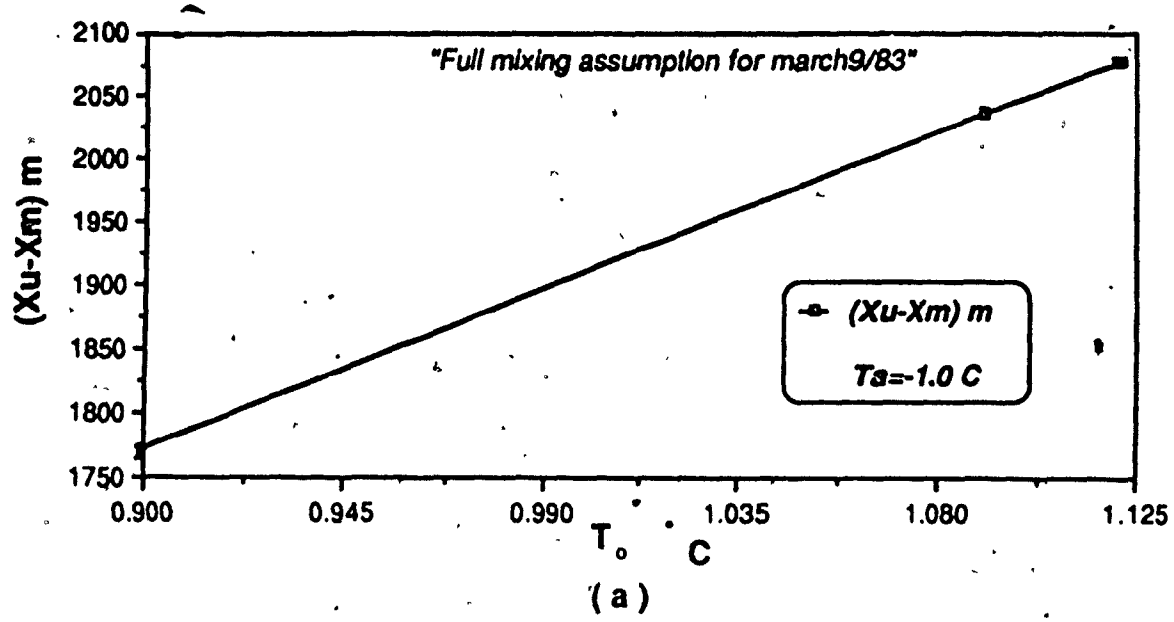

(a)

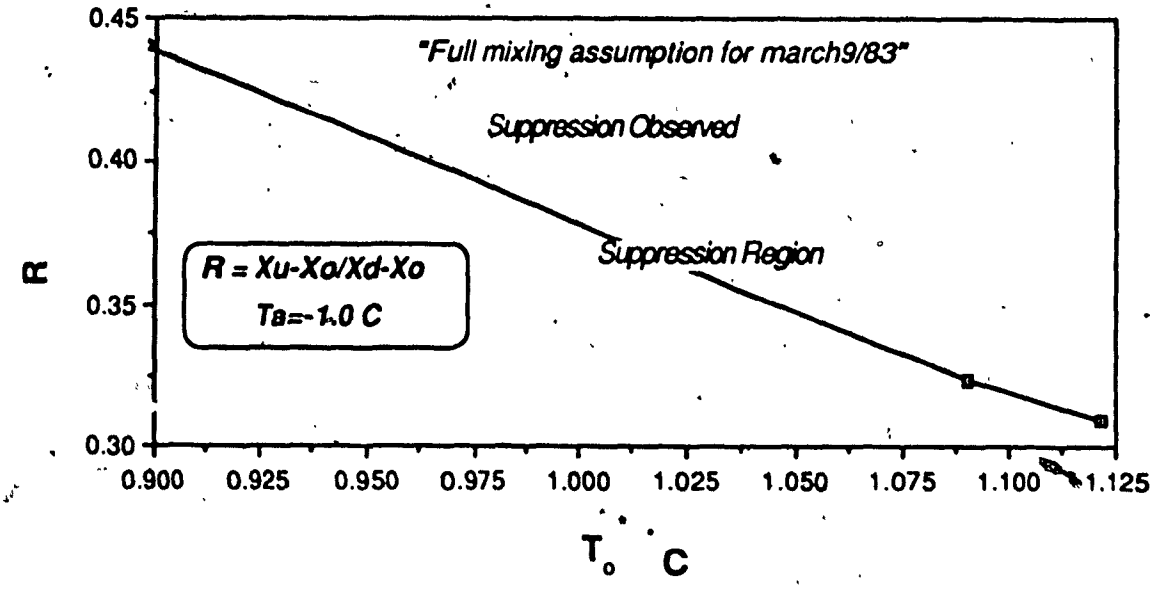

(b)

Fig. (5.3) Calculated ice cover conditions with full mixing assumption:

a) upstream ice edge; b) suppression ratio for March 9,1983.

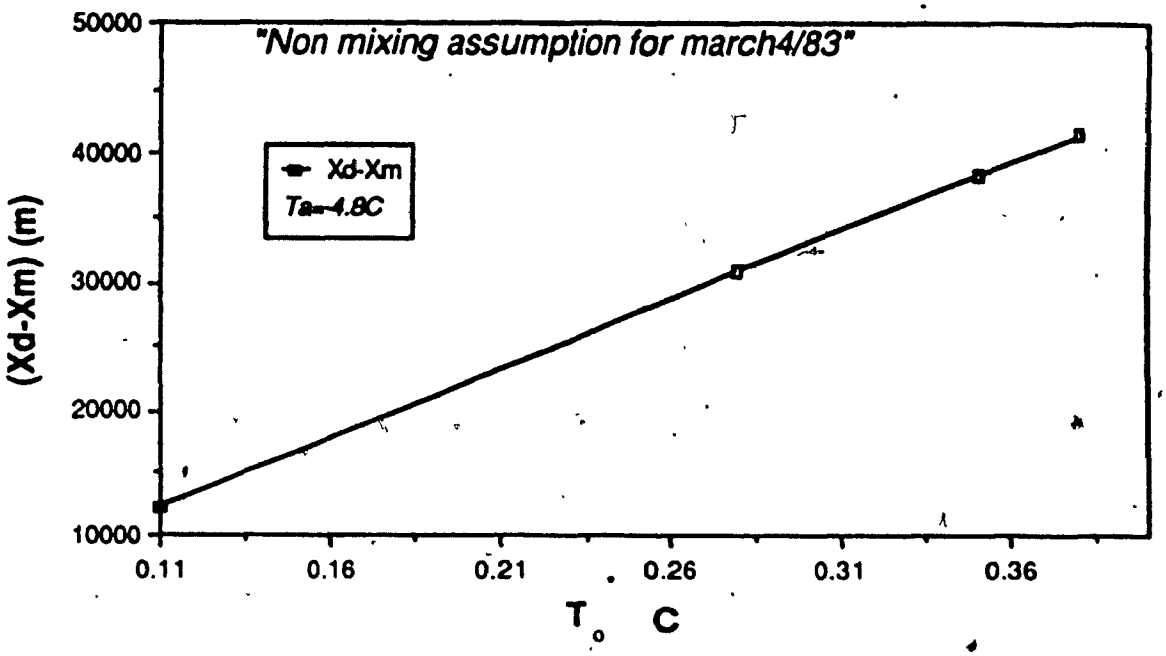

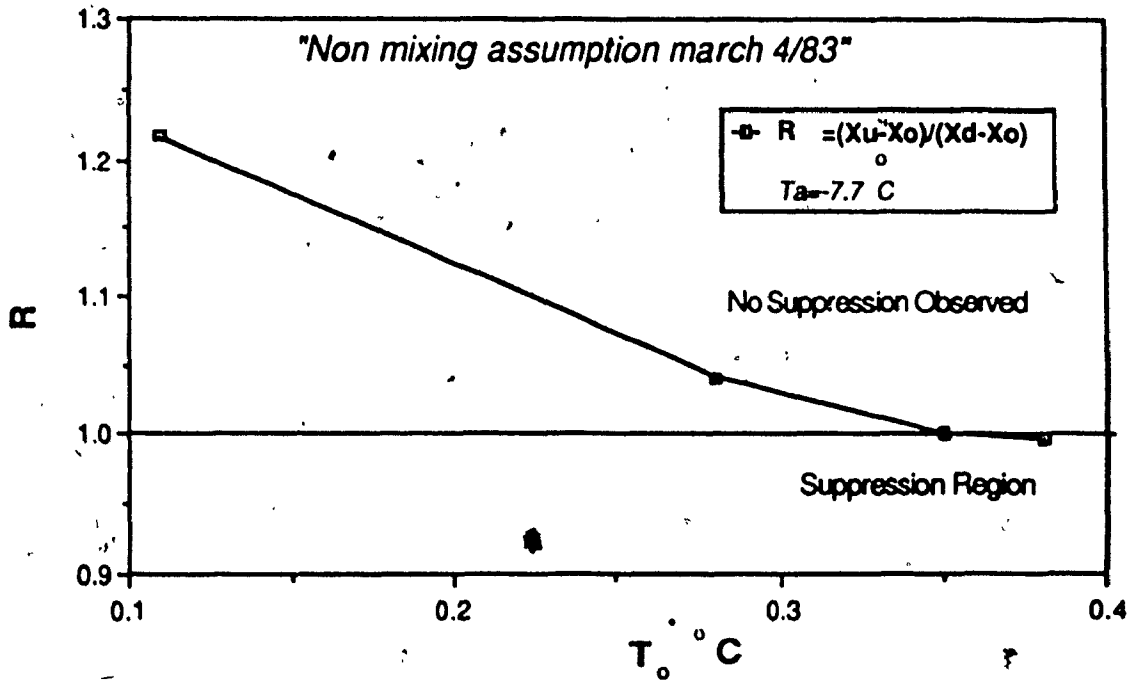

Fig. (5.4) Calculated ice cover conditions with non-mixing assumption:

a) downstream ice edge; b)suppression ratio for March4,1983.

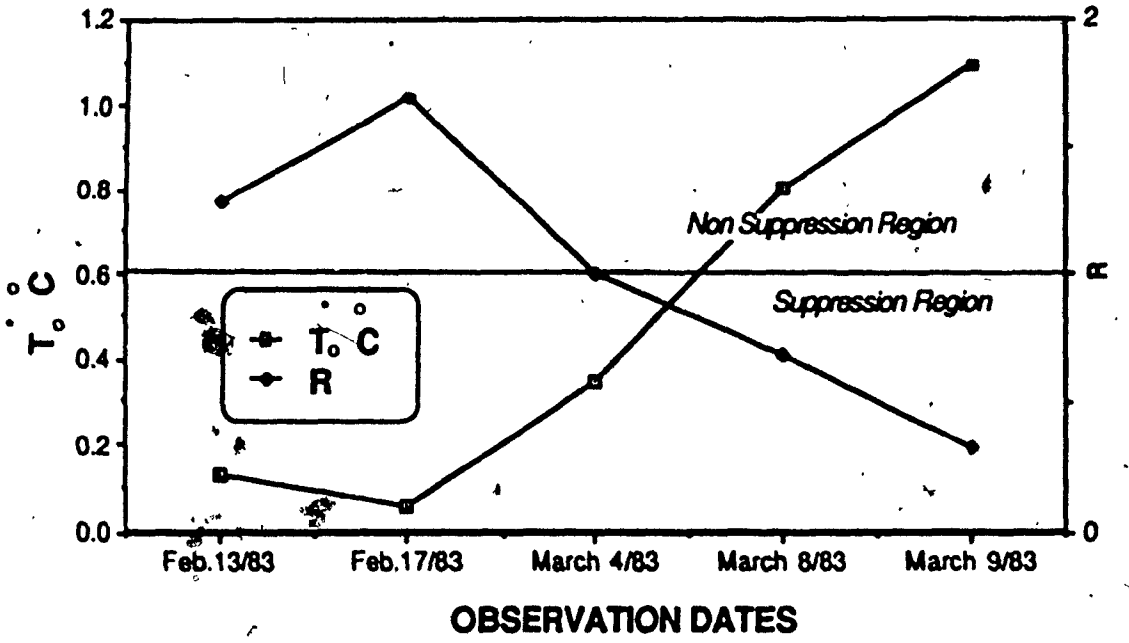

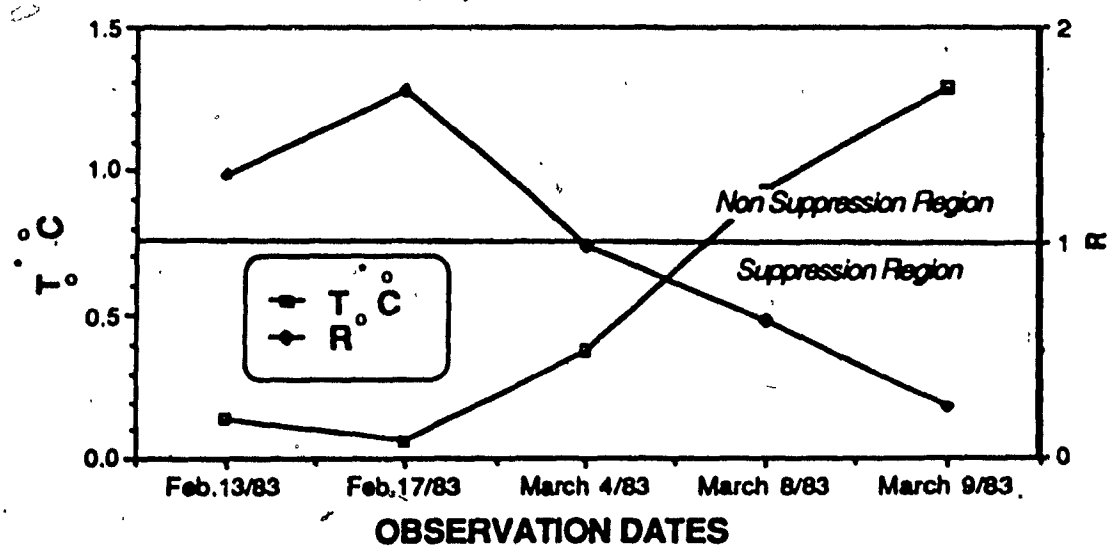

Fig. (5.5) Interrelation between the suppression ratio R and T_o^* for various observation dates for : a) full mixing assumption; b) non-mixing assumption.

CHAPTER VI

CONCLUSIONS

In the present study, the upstream and the downstream locations of the ice edge were investigated for both unsteady uniform flow, as well as for steady non-uniform flow. Ice cover was assumed to exist on the upstream section, and was subjected to suppression in the vicinity of a thermal effluent source. The upstream and the downstream ice edge locations were in agreement with the 0 °C isotherm criterion. It was shown that the effect of the variable velocity is significant, especially on the movement of the downstream ice edge. The new criteria based on the ratio R proved to be practical and accurate in predicting ice cover suppression. Furthermore, the suppression of the ice cover was found to be a function of the flow velocity and of the mixing rate of the thermal effluent discharge.

Chapter-IV provides a general form solution for the one-dimensional quasi-linear energy equation developed herein. Perturbation techniques, based on the WKB(Wentzel, Karmers and Brilloun) approximation and Liouville-Green transformation, were used in the formulations. The effect of flow velocity variability on ice cover suppression has been examined in depth. Also, the above formulations account for the effect of the longitudinal diffusion term. Three practical examples were also shown in the analysis; these examples emphasize the flow velocity as a contributing factor leading to ice cover suppression beside the thermal effluent discharge. The formulation of the upstream distance to the ice edge was not included in the analysis, simply because the upstream flow velocity is negligible and has little effect on the formulation of the problem. However, the above studies were mainly conducted to calculate the downstream ice-free reach based on the 0 °C isotherm criterion. By examining the results shown earlier, and from the figures for the downstream distance to the ice edge for

different flow velocities, whether for constant flow velocity or for diverge and converge channels, we will find that the value of $(x_d - x_m)$ does increase under high velocities, and decrease for low velocities.

Comparison with field data shows the validity of the above formulation as well as of the proposed mixing formula, which take into account the water temperature from the colder upstream of the point of discharge tributaries.

For future investigators who are interested in this subject, it would be desirable to investigate the effect of the flow depth variability on the ice cover suppression, since in rivers of greater depth, the water loses heat more slowly than in shallower rivers, consequently preventing or delaying the ice cover formulation.

REFERENCES

1. ANDERSON, E.R.,1954, "Energy Budget Studies in Water Loss Investigation: Lake Henfer Studies" Technical Report, U.S. Geological Survey Professional Paper 269. pp.71-118.
2. ARDEN, R.S. and WIGLE, T.E., 1972, "Dynamics of Ice Formation in the Upper Niagara River", International Symposia on the Role of Snow and Ice in Hydrology, Banff, Alberta.
3. ASHTON, G.D., 1972a,"Turbulent Heat Transfer to Wavy Boundaries" , Proc. 1972 Heat Transfer Fluid Mechanics Inst., pp. 200-213.
4. ASHTON, G.D., 1978, "River Ice" Ann. Rev. Fluid Mechanics (10): pp. 369-392.
5. ASHTON, G.D., 1979, "Suppression of River Ice by Thermal Effluents." , Parts I and II, USA Cold Regions Research and Engineering Laboratory, CRREL Report, pp. 19-30.
6. ASHTON, G.D., 1980, "Artificial Effects on River Ice", Dynamics of Snow and Ice, pp. 294-303.
7. ASHTON, G.D., 1984, "River Ice Suppression by Side Channel Discharge of Warm Water", IAHR, Montreal, Quebec.
8. ASHTON, G.D., 1986, Personal Communication at the 4th Workshop on Hydraulics of River Ice., June 17-19, Ecole Polytechnique, Montreal.
9. ASHTON, G.D., KENNEDY, J.F., 1970, "Temperature and Flow Conditions During the Formation of River Ice", See. Int. Assoc. Hydraul. Res. Paper 2.4, 12pp.
10. ASHTON, G.D., KENNEDY, J.F., 1972, "Ripples on Underside of River Ice Covers", J. Hydraul. Div. ASCE 98: pp. 1603-24.

11. ASVALL, R.P., 1972, "Change in Ice Conditions in Regulated River Basins", Proc. of Banff Symposia on the Role of Snow and Ice in Hydrology, Banff, Sept. Vol. 2, pp. 1283-1295.

12. CALKINS, D.J., 1984, "Ice Cover Melting in Shallow River", Can. Jnl. Civil Eng. II pp. 225-265.

13. CARTER, H.H., and OKUBO, A. 1972, "Longitudinal Dispersion in Non-uniform Flow", Water Resources Research, Vol. 8, June.

14. CARSTENS, T., 1966, "Experiments with Supercooling and Ice Formation in Flowing Waters", Geofysiske Publikasjoner, Vol. 26, No.9, pp.1-18.

15. CARSTENS, T., 1970, "Heat Exchange and Frazil Formation" Proc. of IAHR Symposium on Ice and Its Action on Hydraulic Structures, Sept., Reyjavik, Paper 2.11.

16. DINGMAN, S.L., 1972, "Equilibrium Temperature of Water Surface as Related to Air Temperature and Solar Radiation", Water Resources Research, Vol. 8, No.1, Feb.

17. DINGMAN, S.L., WEEKS, W.F. and YEN, Y.C., 1967, "The Effect of Thermal Pollution on River-Ice Conditions", Part 1. United States Army Cold Regions Research and Engineering Laboratory, Hanover, N.H. Dec.

18. DAILY, J. A., ROBINSON, P. J., HARLEMAN, D. R. F.,1966, Fluid Dynamics, Addison-Wesley Publishing Co., Reading, Mss.

19. ENGMAN, E.O., 1977, "Turbulent Diffusion in Channels with a Surface Cover", Hydraul. Res., Vol.15, No. 4, pp. 327-335.

20. EDINGER, J.E., DUTTWEILER, D.W., and GEYER, J.C. 1968, "The Response of Water Temperature to Meteorological Conditions", Water Resources Research, Vol. 4, Oct.

21. EDINGER, J.E. and GEYER, J.C., 1965, "Heat Exchange in the Environment", Publication

No. 65-902, Edison Electric Institute, New York, June.

22. INCE, S . and ASHE, G.W.T.1964, "Observations on the Water Temperature Structure of the St-Lawrence River, Proceedings of the Eastern Snow Conference pp. 1-13.

23. FREYSTEINSSION, S., 1970, "Caculation of Frazil Ice Production", Int. Ass. HYD. Res., Paper 2.1, pp. 188-192.

24. FISCHER, H.B., 1967, "The Mechanics of Dispersion in Natural Streams", Jnl. of Hydraulic Div, Proc. of ASCE.

25. FISCHER, H.B.,1973, "Longitudinal Dispersion and Turbulent Mixing in Open Channel Flow", Annual Review of Fluid Mechanics, Vol. 5.

26. HARLEMAN, D.R.F.,1972, "Longitudinal Temperature Distribution in Rivers and Estuaries; One Dimensional Mathematical Models", Engineering Aspects of Heat Disposal from Power Generation. MIT Summer Session, June.

27. HAYNES, F.D. and G.D. ASHTON, 1985, "River Ice Suppression by Thermal Discharges", Preliminary Report No. 32289, CRREL, Hanover, N.H.

28. JOBSON, H.E., and YOTSUKURA, N. 1972, "Mechanics of Heat Transfer in Non-Stratified Open Channel Flows," Institute of River Mechanics Paper, Colorado State Uinversity, Aug.

29. NYFEH, A.H., 1982, "Introduction to Perturbation Techniques ", Jone Willy, New York.

30. NYFEH, A.H., 1985, Problems in Perturbation, Jone Willy, New York.

31. PAILY, P.P., 1974, "Winter-Regimes Thermal Response of Heated Streams", Thesis submitted in partial fulfillment of the requirements for the degree of Doctor of Philosophy in the Dept. of Mechanics and Hydraulics in the Graduate College of the University of Iowa.

32. PAILY, P.P., MACAGNO, E.O. and KENNEDY, J.F., 1974, "Winter-Regime Surface Heat

Loss from Heated Streams", Iowa Institute of Hydraulic Research Report, Iowa City, Iowa. No.155, Feb.

33. ROHSEN, W.M. and H.Y CHOI, 1961, Heat Mass and Momentum Transfer, Englewood Cliffs, N.J., Prentice Hall Inc.

34. SAYER, W.W. 1970, "Natural Mixing Processes in Rivers", Paper Presented at The Conference on "Shall We Survive a Confrotation With Pollution," University of Iowa, April,

35. SILBERMAN, E., 1974, "Discussion of Paily, Macagno, E.O. and Kennedy", ASCE.

36. SARRAF, S. and SALEH, W. 1987, "Local Melting of Ice Cover By Thermal Side Effluent", Submitted to The Cold Region Engineering, ASCE.

37. SARRAF, S., 1987, "Analysis of Heat Induced Suppression of Ice Cover, Using Perturbation". Submitted to The Water Resources Research.

38. SALEH, W. SARRAF, S. and MARCOTTE, N. 1987" Local Suppression of River Ice Cover Due to A Side Effluent" .8th Canadian Hydro-Technical Conferance. Montréal Québec.

39. SALEH, W. et al. 1986. " The Effect of A Tributary Effluent on Ice Cover Progression" 4th Workshop on Hydraulics of River Ice. Montréal Québec.

40. WEEKS, W.F., KEELER,C.M., PARROTT, W. and LEVINE, D.,1971,"Wintertime Dissipation of Heat from a Thermally Polluted River", Water Resources Research Vol.7.

41. YOTSUKURA, N., JACKMAN, A.P., and FAUST, C.R. 1983, "Approximation of Heat Exchange at the Air-Interface ", Water Resources Research, Vol. 9, Feb..

42. " Campagne de mesures de glaces" 1982-83, Hydro-Québec, Annexe (C) Prepared by Recherches B. C. Michel Inc.

APPENDIX

TABLE 2.1

TOTAL HEAT LOSS RATES AT WATER SURFACE

Cloud Coverage	Wind Speed	Heat Loss Rate cal cm^{-2} hr^{-1} Air Temperature ^{o}C			
0-10	m s-1	0	-10	-20	-30
0	1	11.9	24.1	34.6	45.4
	5	12.6	33.5	51.6	67.5
5	1	6.9	19.1	29.5	40.4
	5	7.6	28.9	46.5	62.4
10	1	2.2	14.1	24.8	35.6
	5	2.9	23.8	41.8	57.7

(Asvall, 1972)

TABLE 2.2

EXPERIMENTAL MEASUREMENTS OF LONGITUDINAL DISPERSION IN OPEN CHANNELS
(AFTER FISCHER, 1973 [20])

Reference	Channel	Depth h (cm.)	Width b (m.)	Shear Velocity u (cm/sec.)	Observed Dispersion Coefficient E (m^2/sec.)	C = E/hu*	E Predicted (m^2/sec.)
Thomas (1958)	Chicago Ship Canal	807	4.8	1.91	3.0	20	
State of Calif. (1962)	Sacramento River	400		5.1	15	74	
Ownes et al. (1964)	River Derwent	25		14	4.6	131	
Glover (1964)	South Platte River	46		6.9	16.2	510	
Schuster (1965)	Yuma Mesa A Canal	345		3.45	0.75	8.6	
Fischer (1967a)	Trapezoidal Laboratory Channel with roughened sides	3.5	.40	2.02	.123	174	.131
		4.7	.43	3.59	.253	150	.251
		3.5	.40	3.51	.415	338	.371
		3.5	.34	3.48	.250	205	.250
		2.1	.33	3.28	.400	392	.450
		2.1	.19	3.88	.220	270	.166
Fischer (1968a)	Green-Duwamish River, Washington	110	20	4.9	6.5 to 8.5	120 to 160	7.8
Yotsukura et al.	Missouri River	270	200	7.4	1500	7500	
Godfrey and Frederick (1970) (Predicted Values of E from Fischer, 1968b)	Copper Creek, Va. (below gage)	49	16	8.0	20	500	6.0
		85	18	10.0	21	250	28
		49	16	8.0	9.5	245	11.4
	Clinch River, Tenn.	85	47	6.7	14	235	15
		210	60	10.4	54	245	11.4
		210	53	10.7	47	210	55
	Copper Creek, Va. (above gage)	40	19	11.6	9.9	220	2.8
	Powell River, Tenn.	85	34	5.5	9.5	200	9.1

TABLE 2.2 (CONT'D)

Reference	Channel	Depth h (cm.)	Width b (m.)	Shear Velocity u (cm/sec.)	Observed Dispersion Coefficient E (m^2/sec.)	C = E/hu*	E Predicted (m^2/sec.)
	Clinch River, Va.	58	36	4.9	8.1	280	30
	Coachella Canal, Calif.	156	24	4.3	9.6	140	3.9
Fukuoka (1971)	Sinuous rectangular Laboratory Channel smooth sides, smooth and rough bottoms - 25 experiments	2.3 to 7.0	.13 to .25	1.1 to 2.7	to	5.8 to 35	to

TABLE 3.1: COMPARISON BETWEEN CALCULATION AND OBSERVATION
(non-mixing assumption)

Date	T_o (°C)	$X_d - X_m$ (km)	$X_u - X_m$ (m)	R Calculated	Observations
Feb.13/83	0.14	9.683	49.1	1.288	no suppression
Feb.17/83	0.06	4.225	21.4	1.697	no suppression
March.4/83	0.28	30.860	156.5	1.040	no suppression
March.8/83	0.93	216.860	1099.5	0.642	suppression
March.9/83	1.29	450.989	2287.2	0.239	suppression

TABLE 3.2: DISCHARGE FIELD DATA

Section	Distance (m)	Q(m^3/s) 14.Feb.83	Q(m^3/s) 17.Feb.83	Q(m^3/s) 4.March.83	Q(m^3/s) 8.March.83	Q(m^3/s) 9.March.83
1	0	247.71	183.86	326.52	343.41	370.69
2	1635	247.71	183.86	326.52	343.41	370.69
3	4085	247.71	183.86	326.52	343.41	370.69
4	5685	1437.45	1931.07	2112.56	2280.51	2084.65
5	7785	8477.28	9099.48	9176.56	9222.41	9129.27
6	9885	8477.28	9099.48	9176.56	9222.41	9129.27

TABLE 5.1a: COMPARISON BETWEEN CALCULATION AND OBSERVATION (full mixing assumption)

Date	T_o^* (°C)	$X_d - X_m$ (km)	$X_u - X_m$ (m)	R Calculated	Observations
Feb.13/83	0.13	9.595	47.5	1.288	no suppression
Feb.17/83	0.055	4.185	20.2	1.697	no suppression
March.4/83	0.35	40.5	205.3	0.996	no suppression
March.8/83	0.803	183.8	973.6	0.686	suppression
March.9/83	1.09	384.31	2035.73	0.3239	suppression

TABLE 5.1b: COMPARISON BETWEEN CALCULATION AND OBSERVATION (non-mixing assumption)

Date	T_o^* (°C)	$X_d - X_m$ (km)	$X_u - X_m$ (m)	R Calculated	Observations
Feb.13/83	0.14	9.683	49.1	1.32	no suppression
Feb.17/83	0.06	4.25	21.4	1.71	no suppression
March.4/83	0.38	41.47	210.3	0.961	no suppression
March.8/83	0.93	216.8	1099.4	0.642	suppression
March.9/83	1.29	451.0	2287.2	0.239	suppression